



Particle Production and Fragmentation

D H Saxon

University of Glasgow

UNIVERSITY
of
GLASGOW

H1 & ZEUS data. New theory.

Charged Multiplicities in DIS and DDIS

Inclusive photoproduction of non-strange mesons

Strange Particle production

Charm fragmentation

Baryons decaying to strange particles

Antideuteron production

KK Bose Einstein correlations

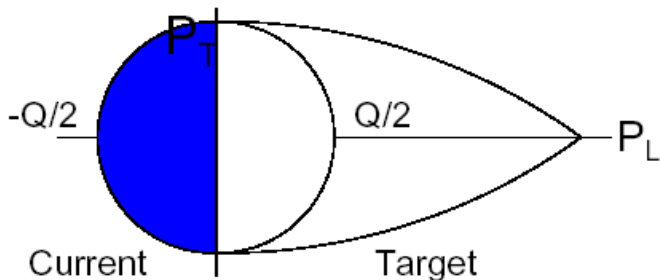
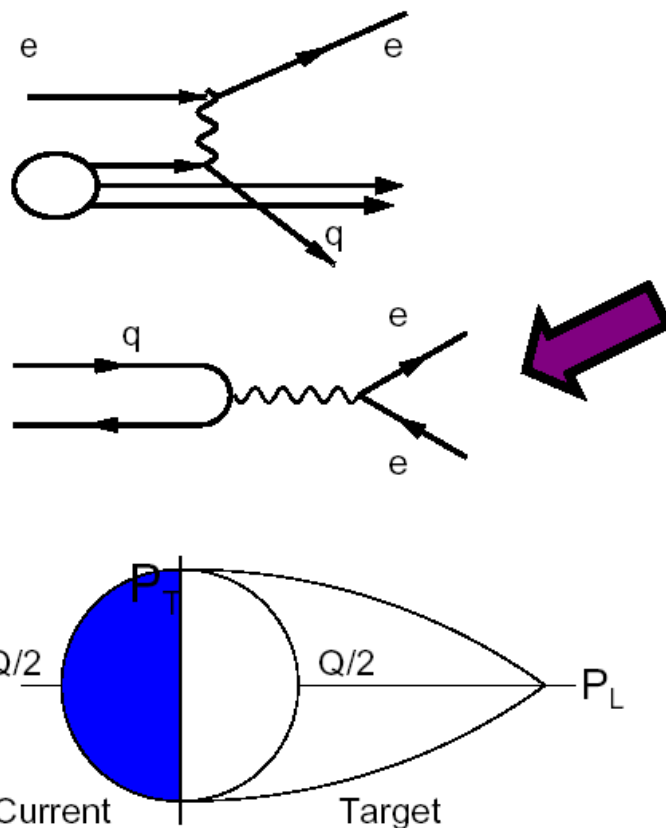
Prompt photon production in DIS

DIS particle multiplicities: use of Breit frame

(De Wolf)

DIS event

Lab Frame Breit Frame



- Use Breit frame to compare multiplicity in ep to (one hemisphere) of e^+e^-

- Breit Frame definition:

$$2xP + q = 0$$

- "Brick Wall frame": incoming quark scatters off photon and returns along same axis.

- Current region (CR) of Breit Frame is analogous to e^+e^- in 0th order pQCD = Quark-Parton Model and energy = $Q/2$

- But: QCD Compton and Boson-Gluon Fusion processes → Particle migration out of current region

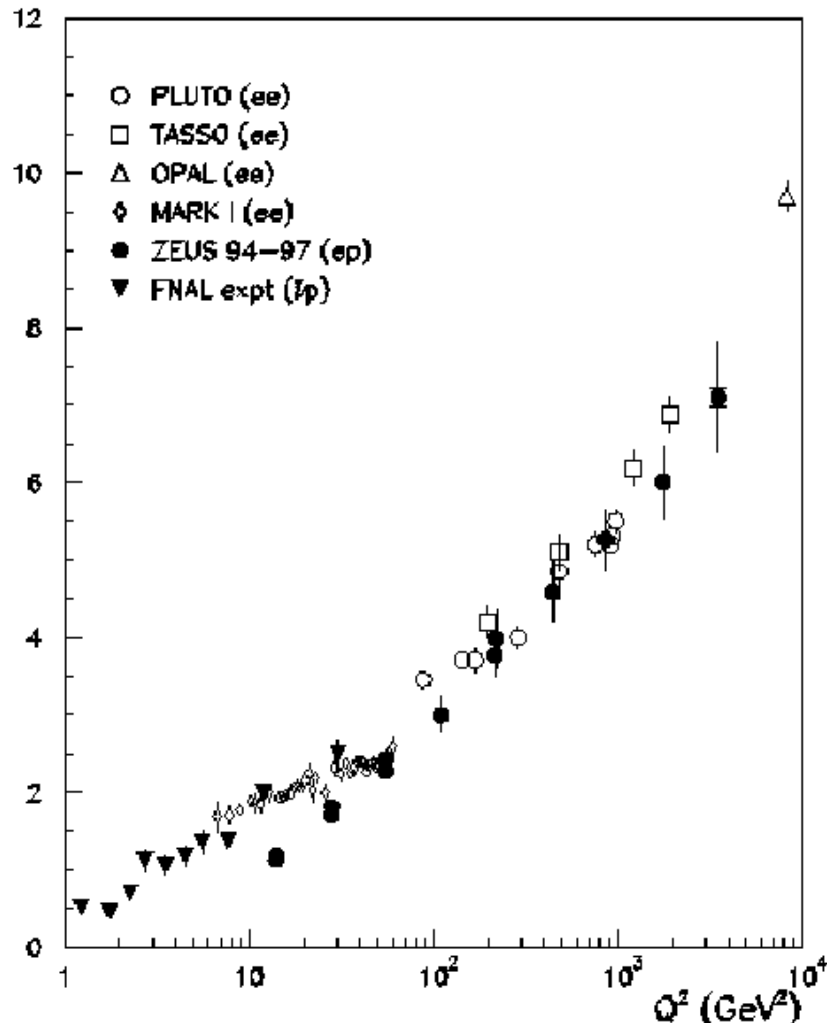
K.H.Streng et al. ZPC 2 (1979) 237; S. Chekanov
J.Phys. G (1999) 59, hep-ph/9806511; 9810477

- Energy in CR < $Q/2$

- **ZEUS:** use measured energy in CR of Breit Frame as energy scale

$\langle n_{ch} \rangle : ep$ (Breit frame) v e^+e^-

ZEUS 1994–97



e^+e^- data divided by 2

Similar within largeish errors at high Q^2

ep result lower at lowest Q^2

Only looking at a fraction of each event.

Can we look at more of each event?

DIS

$$W^2 \sim Q^2/x$$

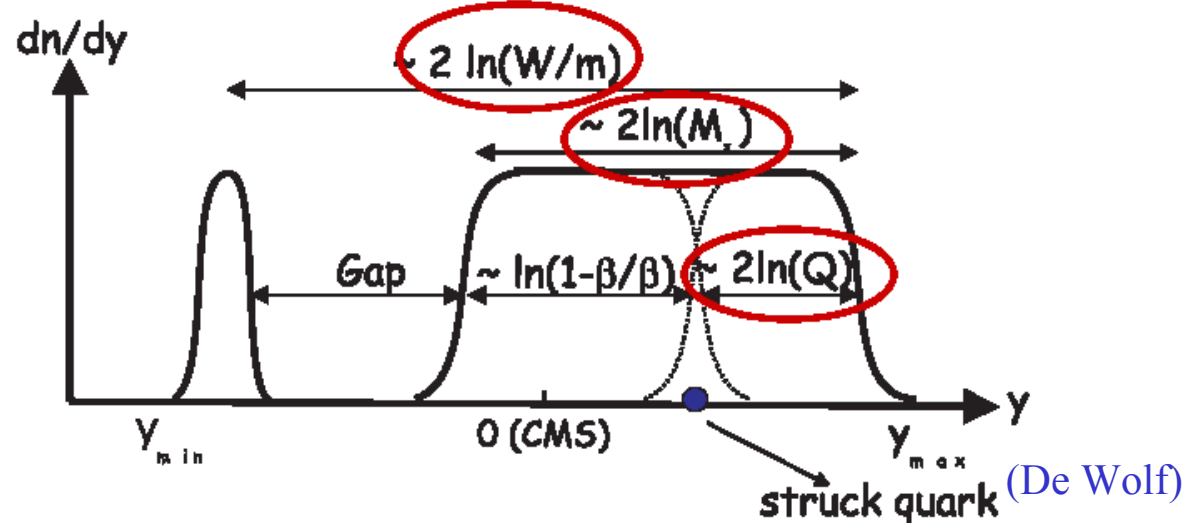
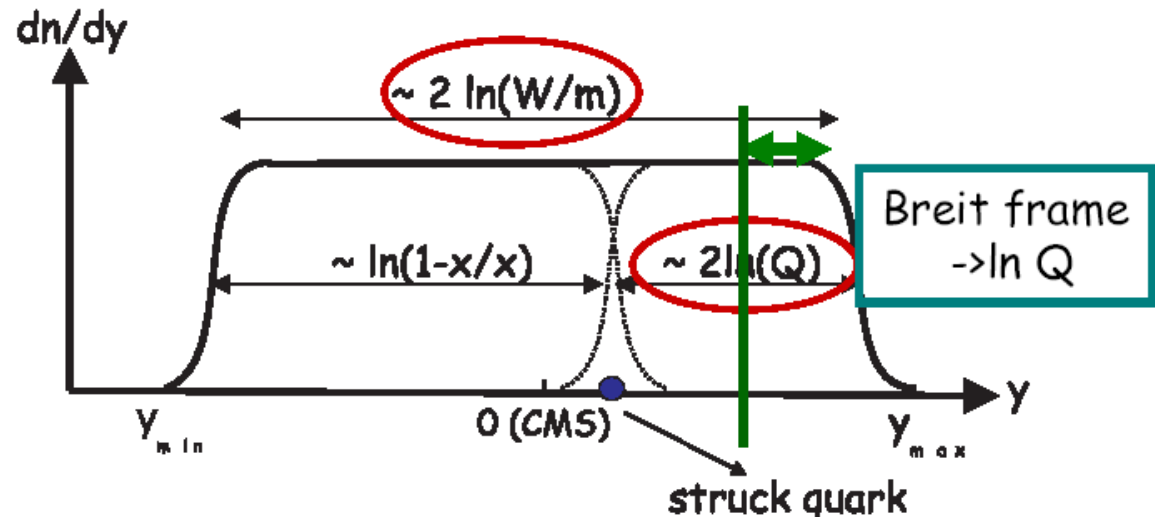
$$y_{\max} = \ln(W/m_\pi)$$

In DDIS β plays role of x in DIS

DDIS

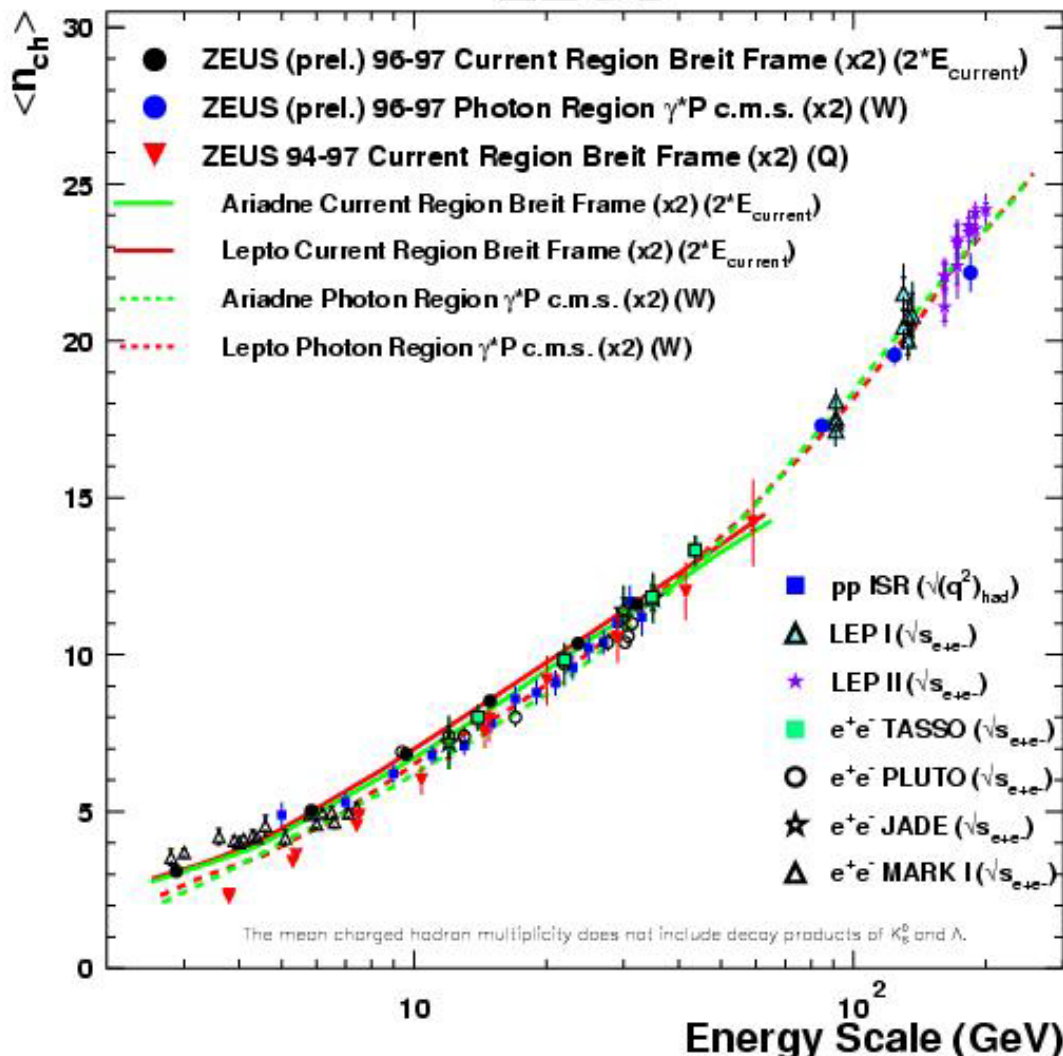
$$M_x^2 = Q^2 \frac{1-\beta}{\beta}$$

$$\text{gap} \sim \ln \frac{1}{x_{IP}}$$



$\langle n_{ch} \rangle : ep$ (Breit, $\gamma^* p$ c.m.s.) v e^+e^- excludes K^0, Λ decay products

ZEUS



$2^* \langle n_{ch} \rangle$ for ep

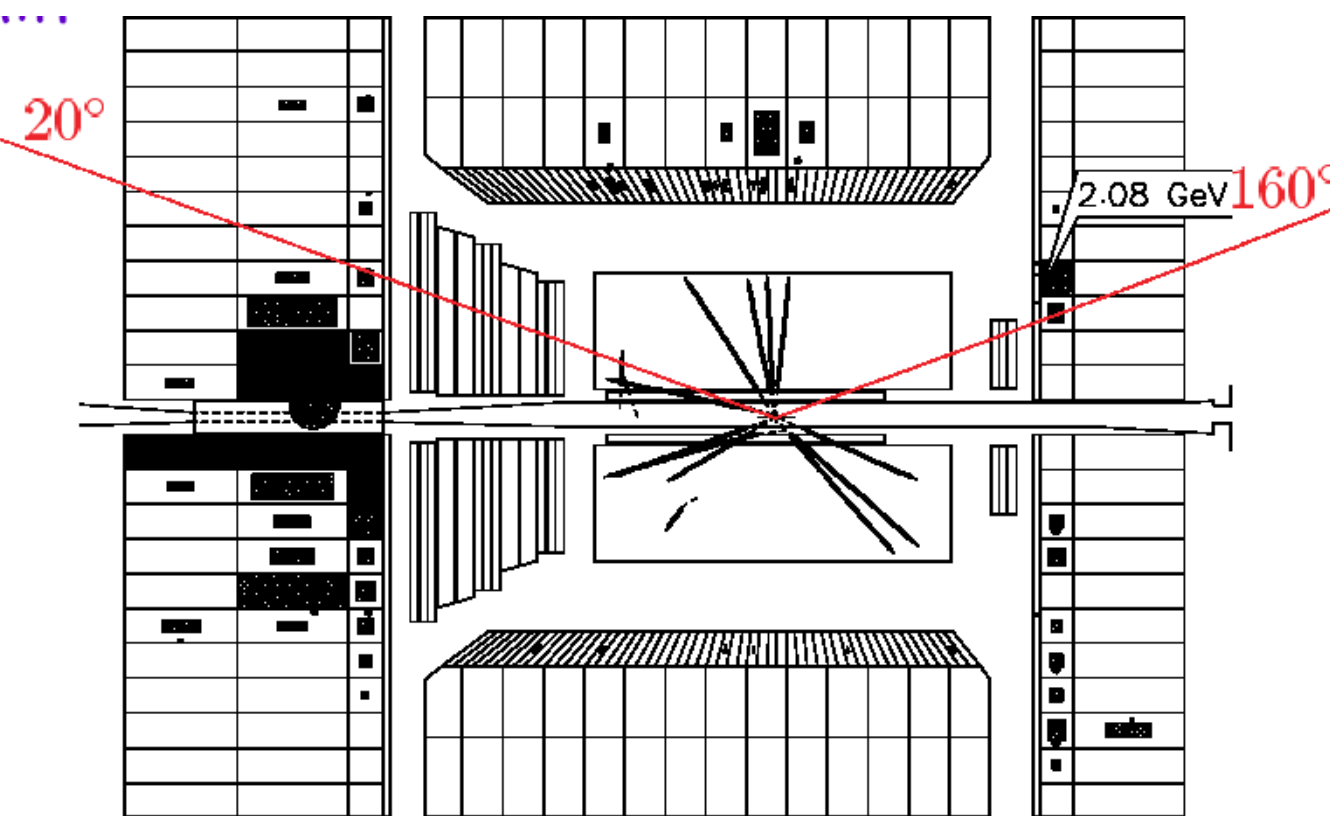
Breit frame:

Closer to e^+e^- if
 $2^* E_{current}$ used as scale
– black dots

$\gamma^* p$ c.m.s. current region:

close to e^+e^- over wide range using W as scale
– blue dots

ZEUS: M_{eff} using best part of central tracker



Exclude scattered electron

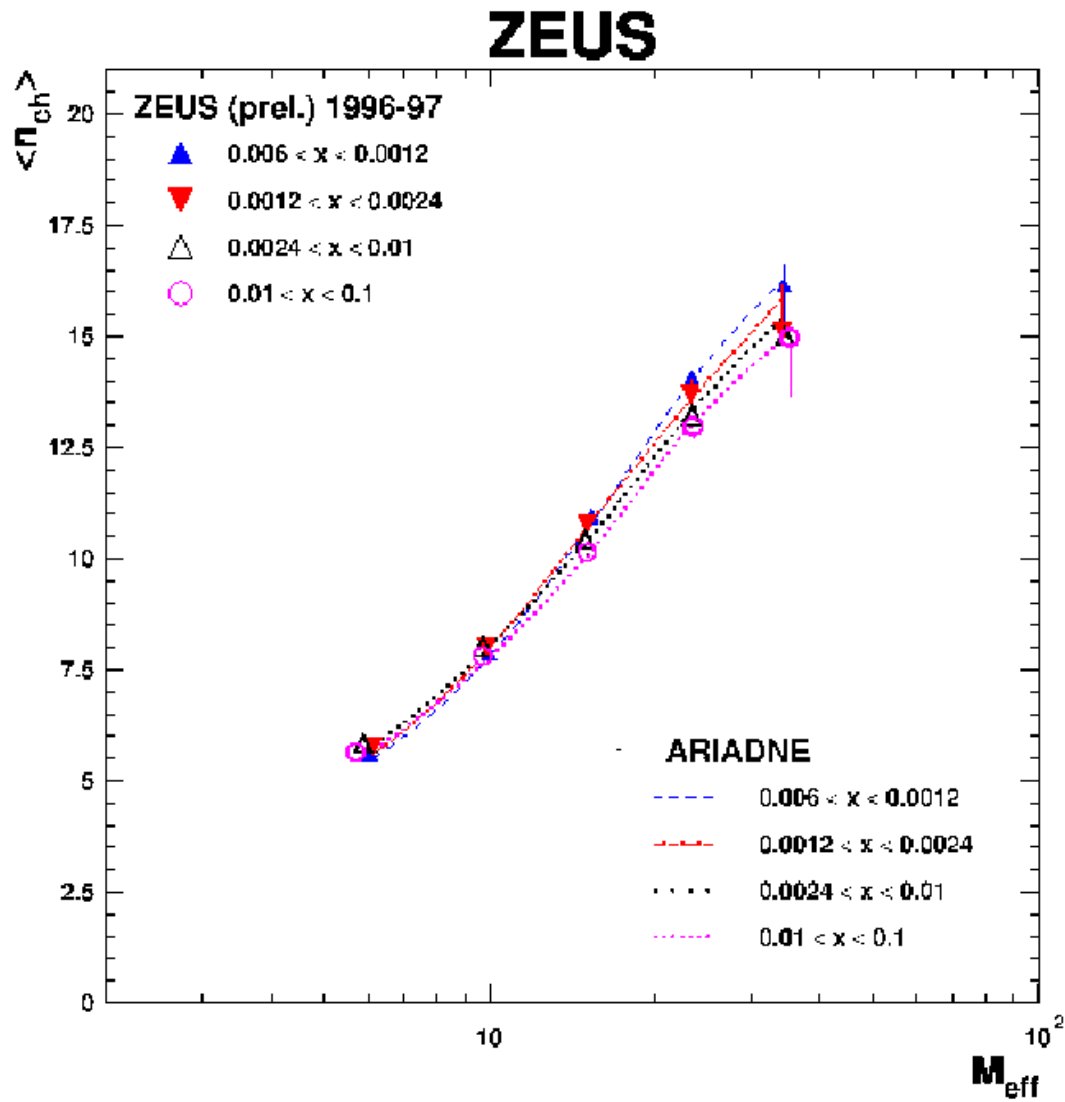
Use best angular range for counting tracks

Use same angular range in calorimeter for

$$M_{eff}^2 = (\sum E)^2 - (\sum \vec{p})^2$$

↑
vector

$\langle n_{\text{ch}} \rangle$ v M_{eff} in x -bins

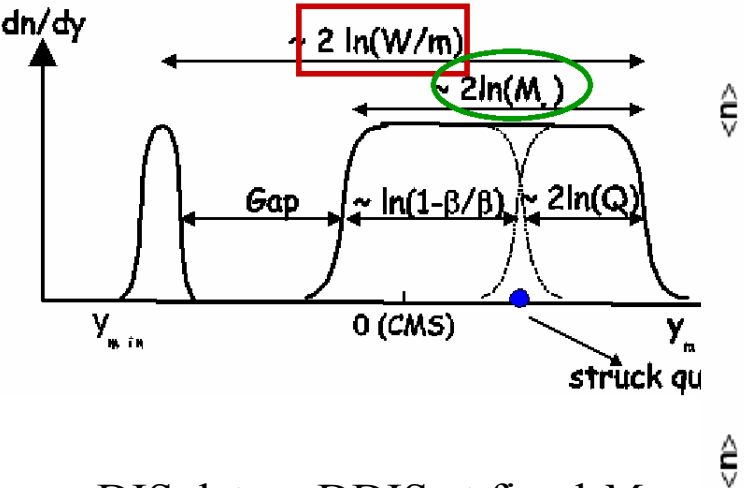


Lab frame
measurement agrees
well with Ariadne

Weak- x_{Bj} dependence

No Q^2 dependence
observed

H1: $\langle n_{\text{ch}} \rangle$ v Q^2 in DIS and DDIS at fixed W

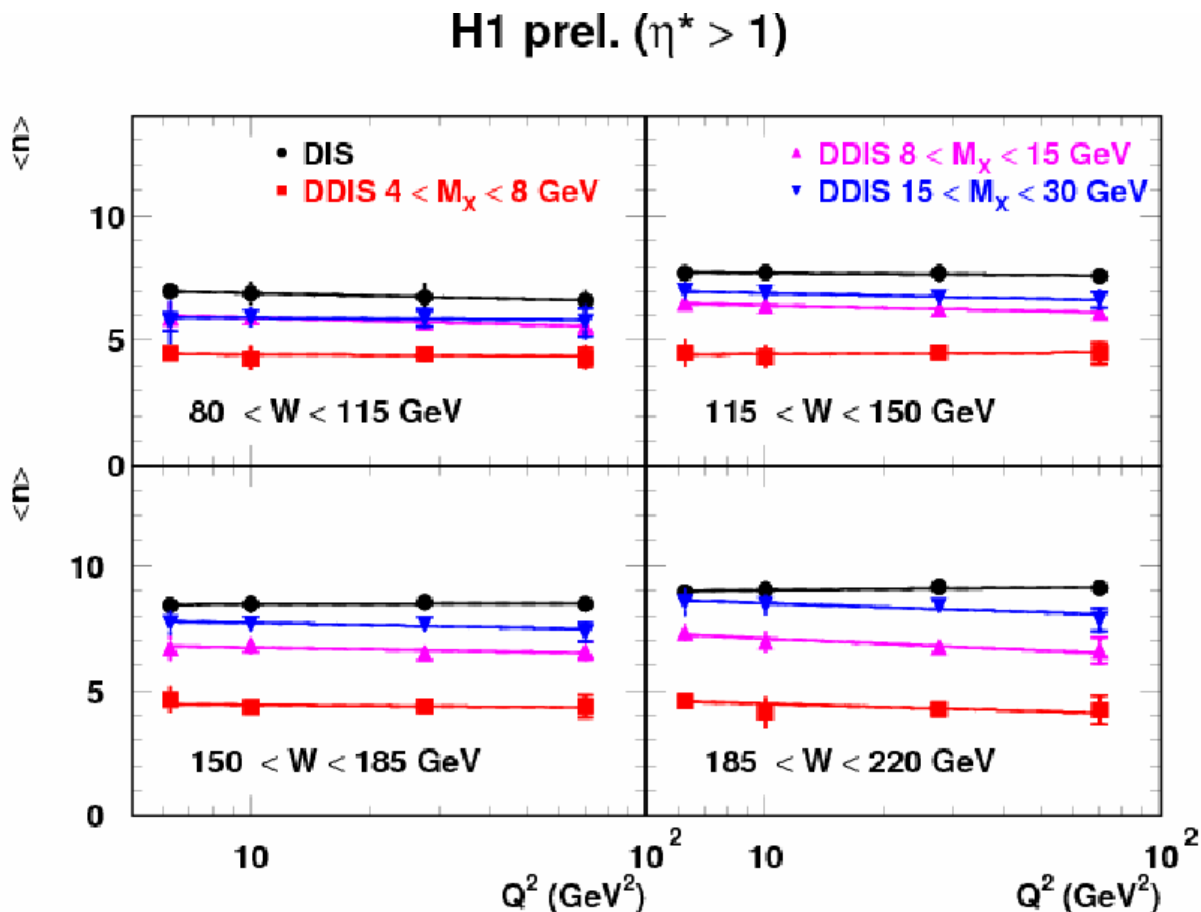


DIS data + DDIS at fixed M_x

No statistically significant dependence on Q^2

Weak W -dependence in DDIS

Rapidity spectra v weak Q^2 dependence (not shown)



$\langle n_{\text{ch}} \rangle$ v W at fixed M_x in DDIS (De Wolf)

H1 Prel. DDIS ($\eta^* > 1$) All Q^2

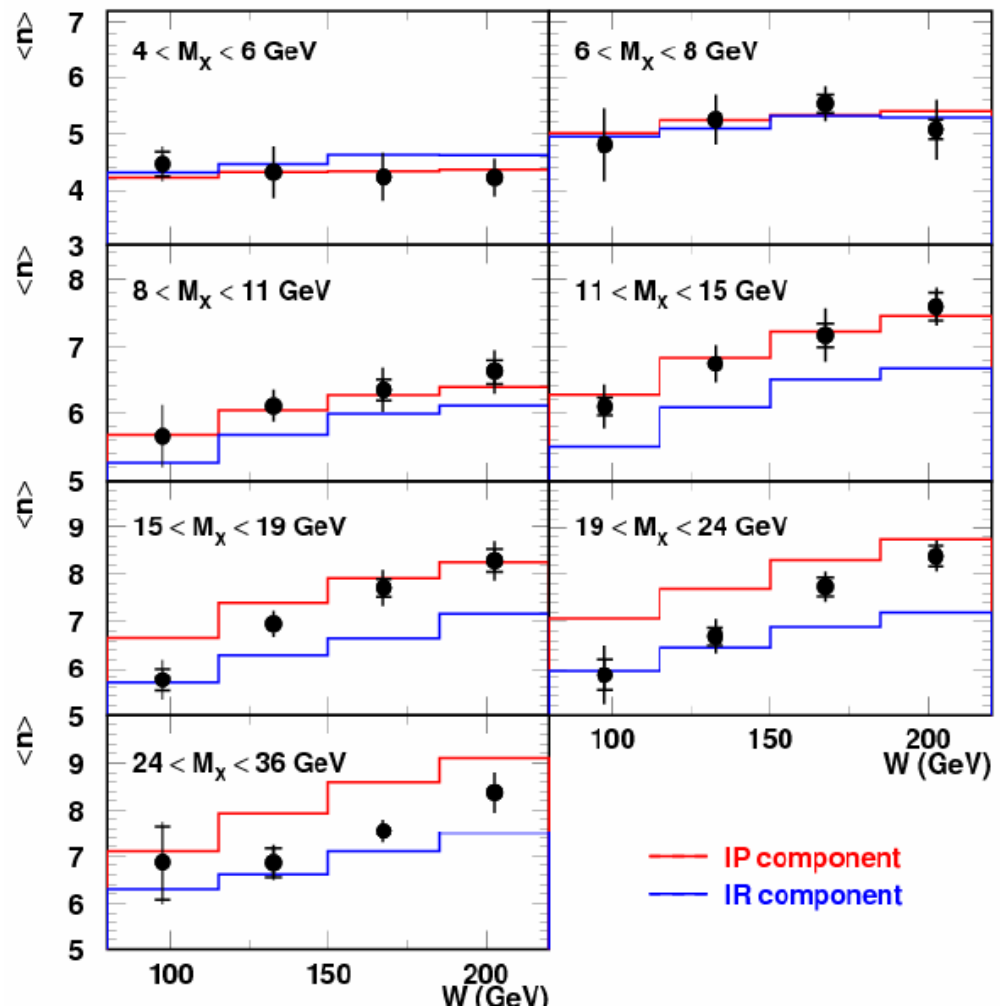
At fixed M_x : changing W means changing gap and x_{IP}

Regge factorization means diffractive pdf's AND Final state properties independent of x_{IP}

W -dependence = breaking of Regge factorization

In resolved Pomeron model: pomeron + reggeon

Large M_x : Data move from Reggeon to Pomeron as W grows

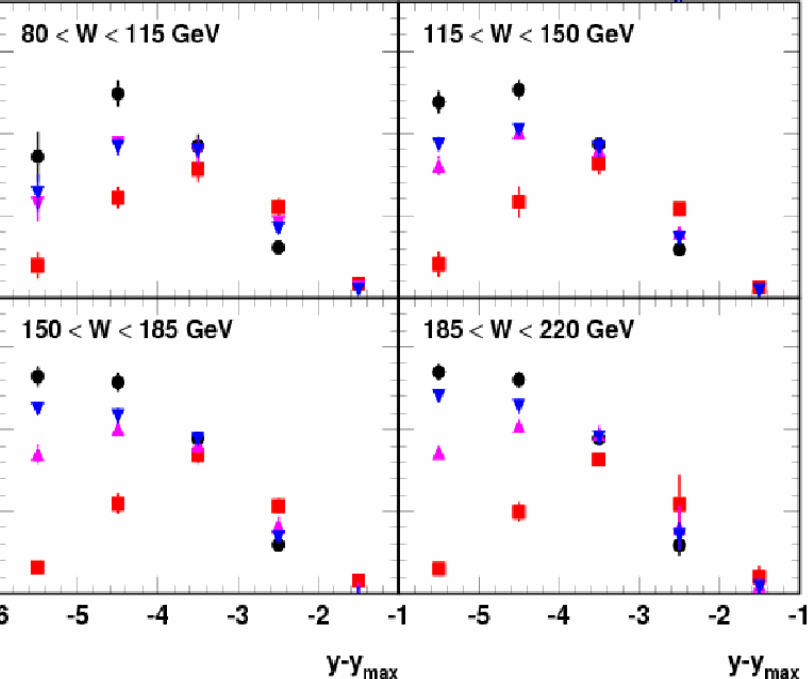


DIS v DDIS: Rapidity distribution

KNO scaling

H1 Prel. ($\eta^* > 1$)

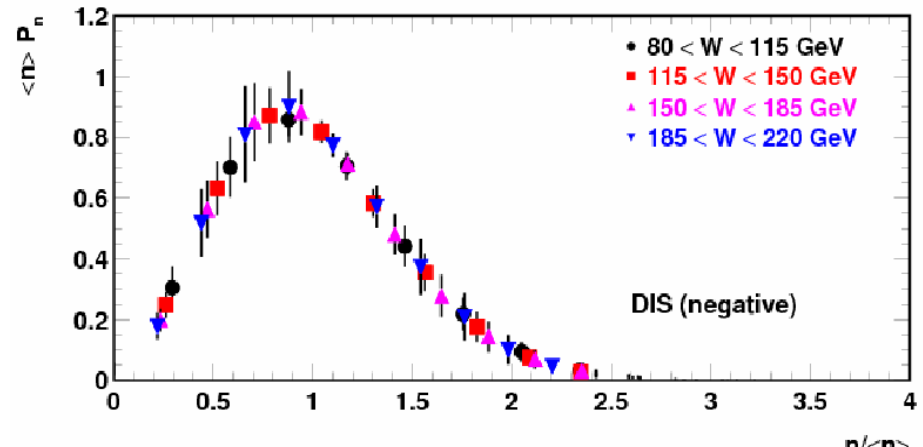
- DIS
- DDIS $4 < M_x < 8 \text{ GeV}$
- ▲ DDIS $8 < M_x < 15 \text{ GeV}$
- ▼ DDIS $15 < M_x < 30 \text{ GeV}$



H1 prel. ($\eta^* > 1$)

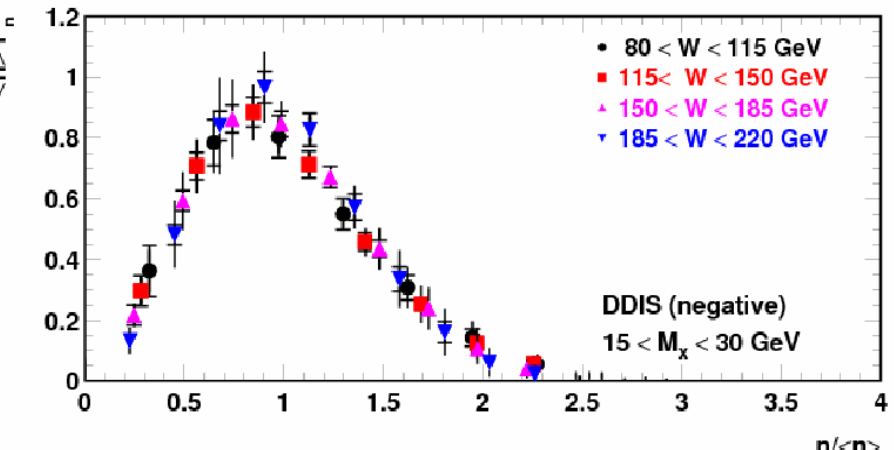
- $80 < W < 115 \text{ GeV}$
- $115 < W < 150 \text{ GeV}$
- ▲ $150 < W < 185 \text{ GeV}$
- ▼ $185 < W < 220 \text{ GeV}$

DIS (negative)



- $80 < W < 115 \text{ GeV}$
- $115 < W < 150 \text{ GeV}$
- ▲ $150 < W < 185 \text{ GeV}$
- ▼ $185 < W < 220 \text{ GeV}$

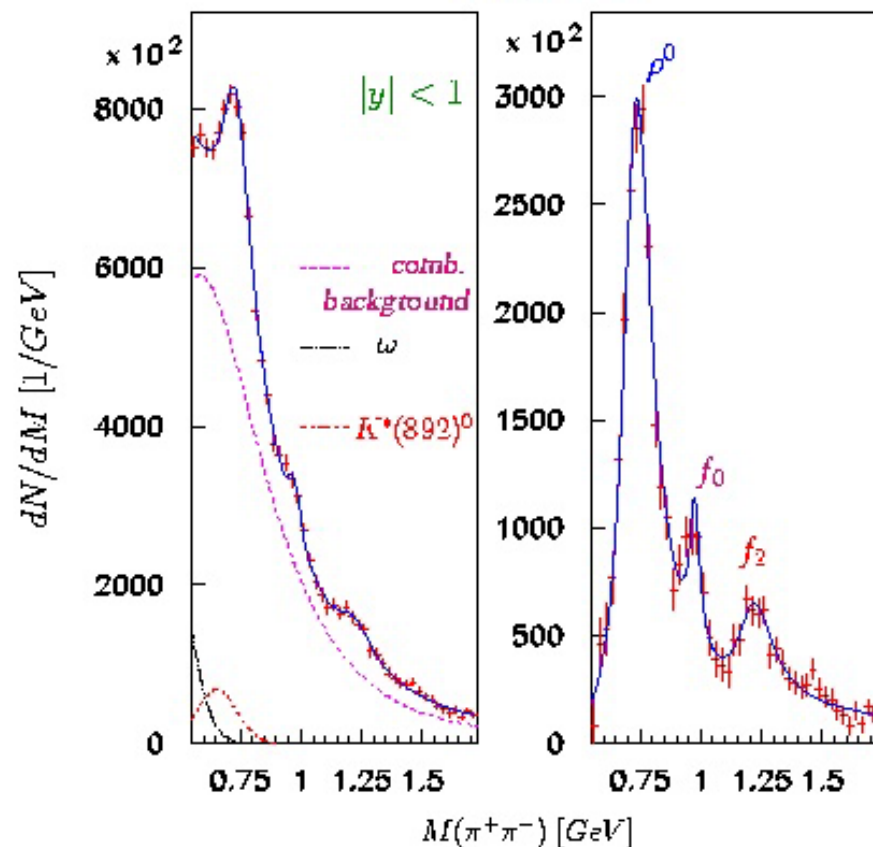
DDIS (negative)
 $15 < M_x < 30 \text{ GeV}$



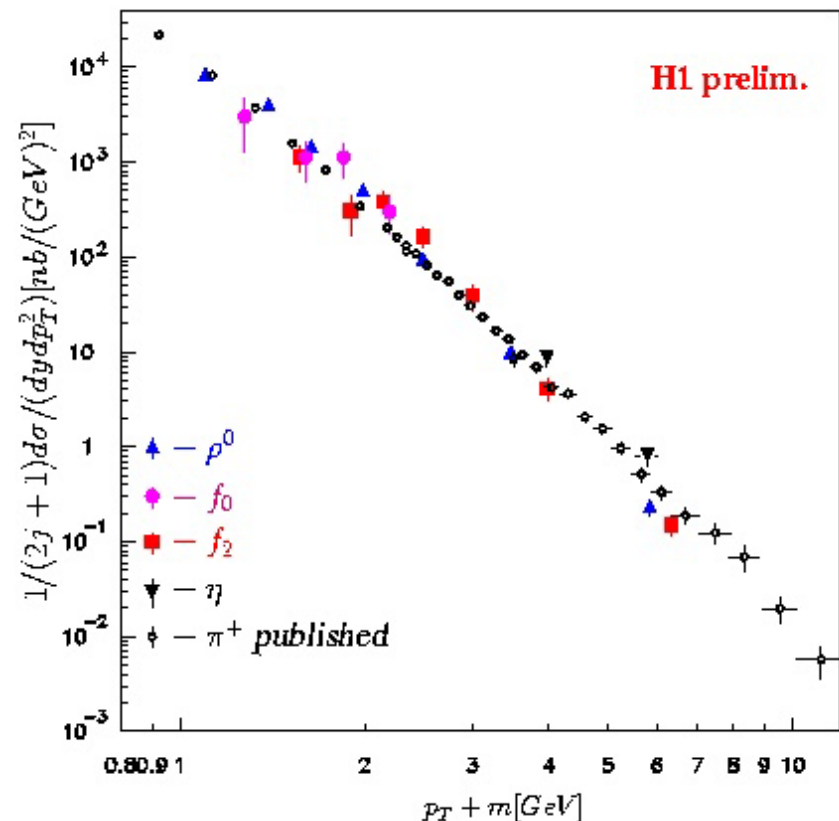
Similar rapidity density at high M_x .
DDIS gluon rich presumably

$\rho^0, f_0, f_2, \eta, \pi^\pm$ inclusive photoproduction

H1 prelim.

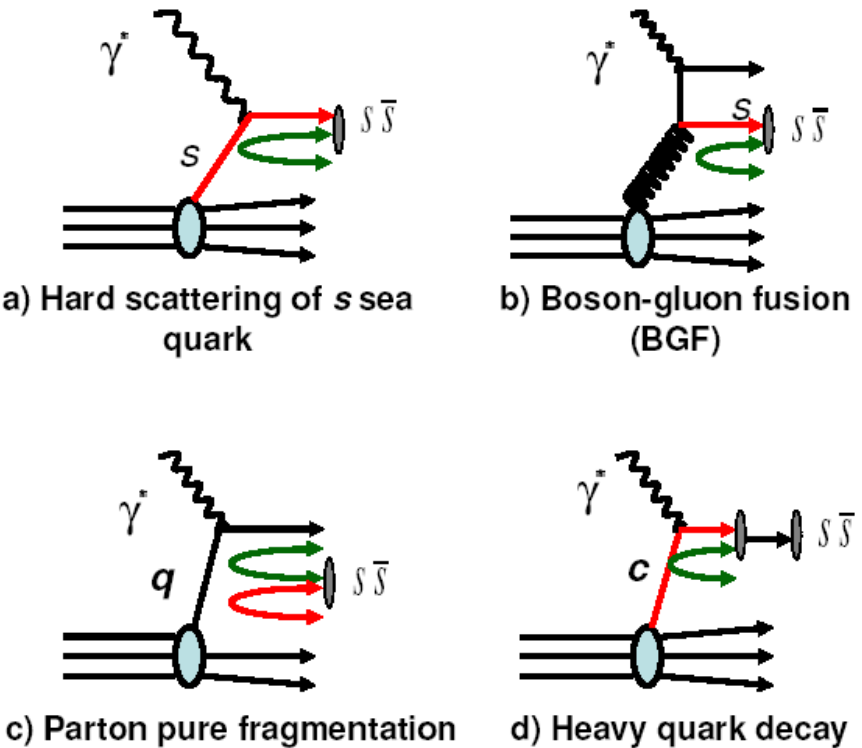
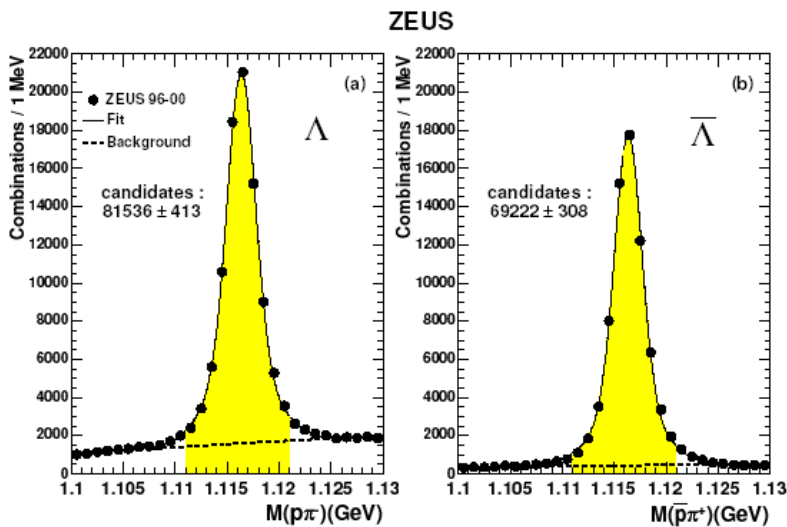
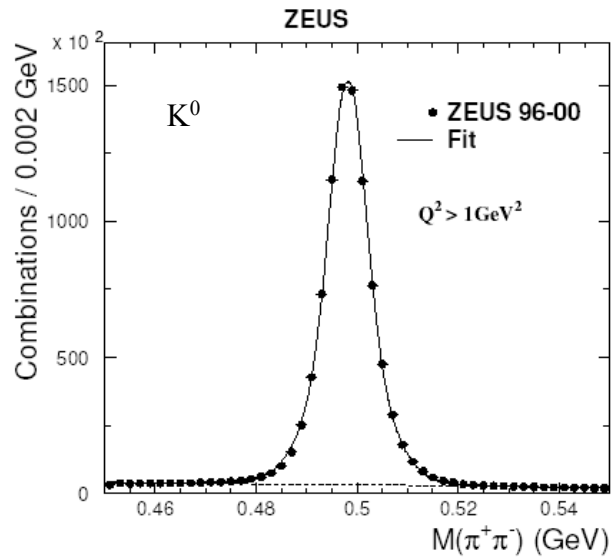


Tricky background & reflection removal



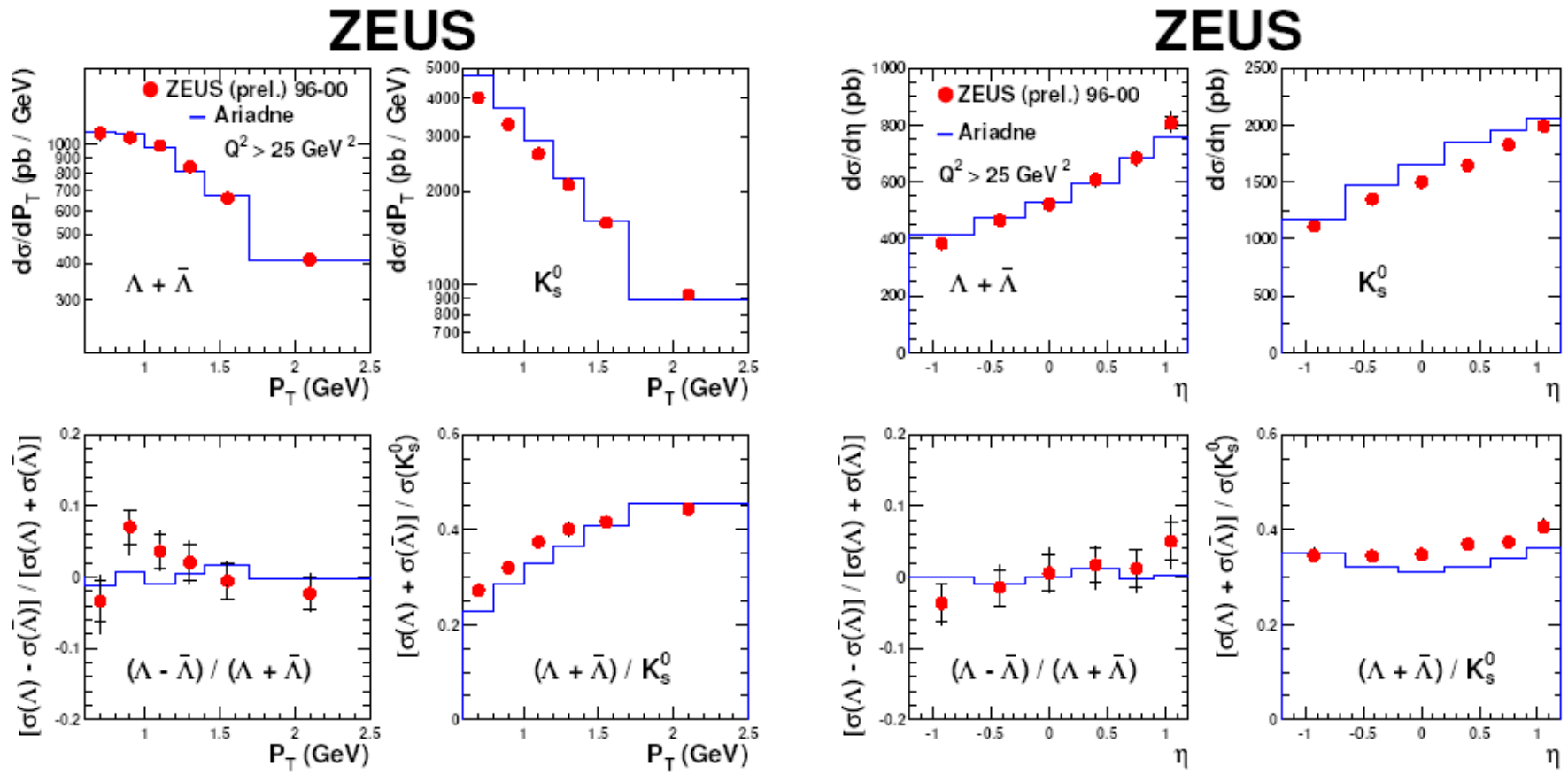
Universal curve plotted against ($p_T + m$)

$K^0, \Lambda^0, \bar{\Lambda}^0$ production



(C Liu)

$K^0, \Lambda^0, \bar{\Lambda}^0 : p_T$ and η

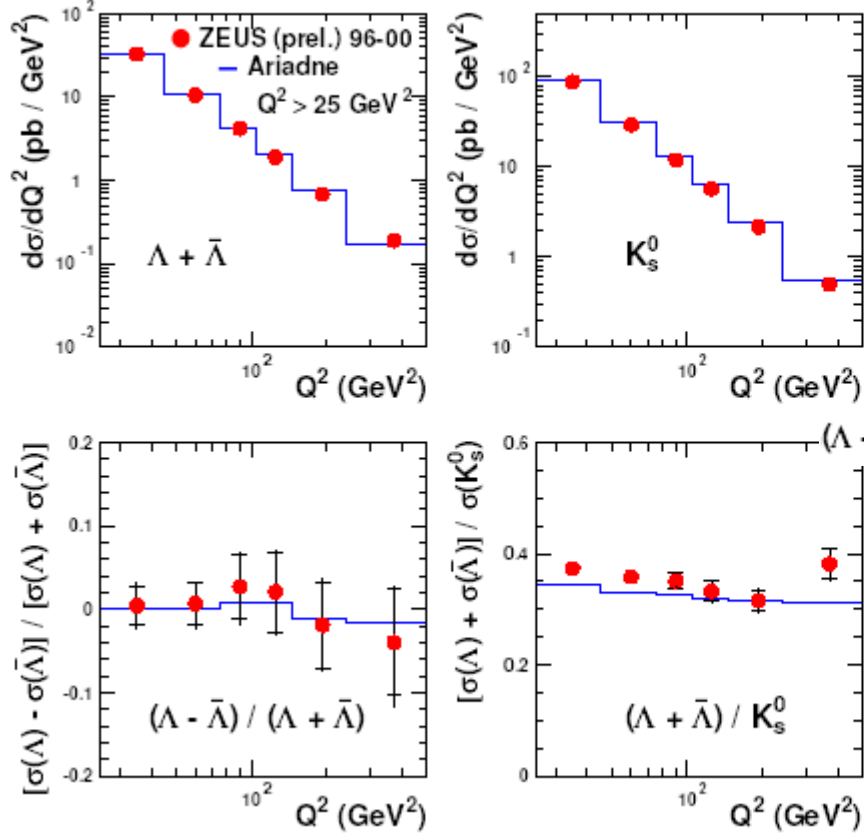


Ariadne mostly OK: overestimates K^0 rate. Favours smaller s/u ratio (0.22?)

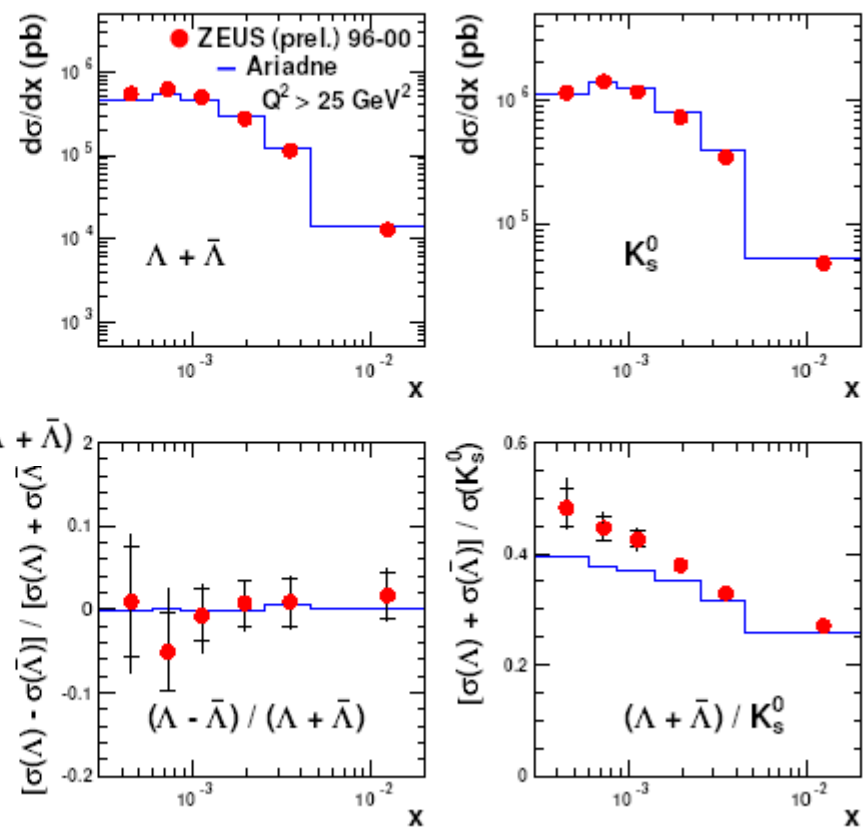
$\Lambda - \bar{\Lambda}$: no significant asymmetry

$K^0, \Lambda^0, \bar{\Lambda}^0 : Q^2$ and x

ZEUS



ZEUS



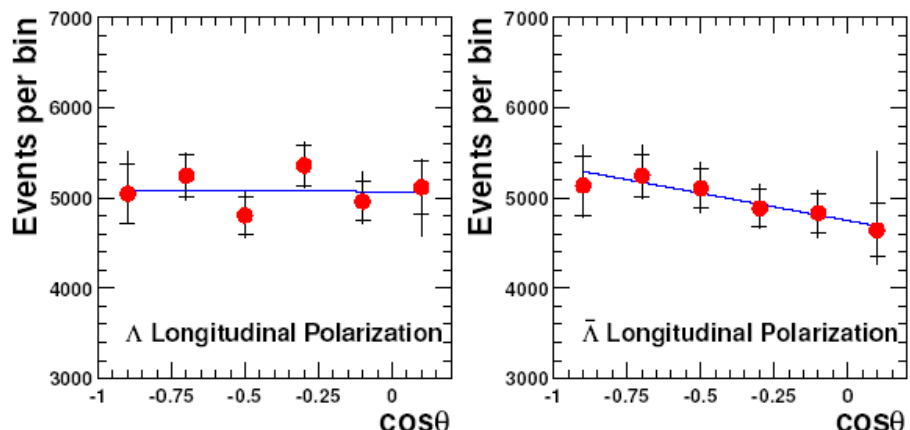
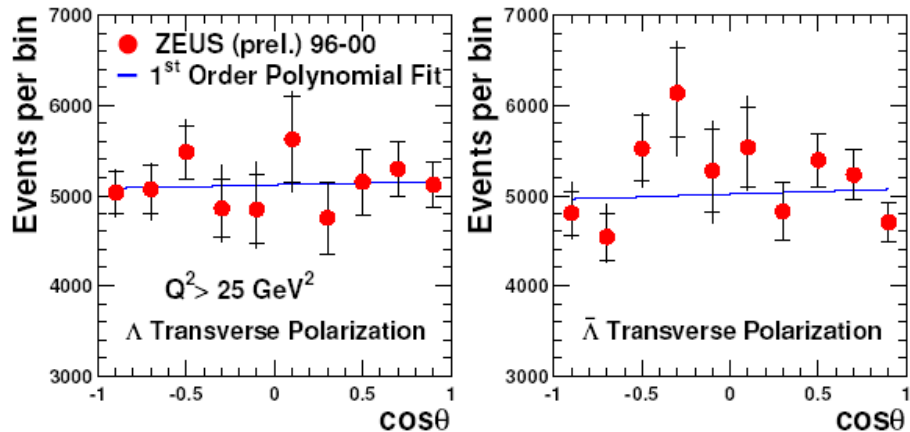
Ariadne: Λ/K poor at low x

$\Lambda - \bar{\Lambda}$: no significant asymmetry

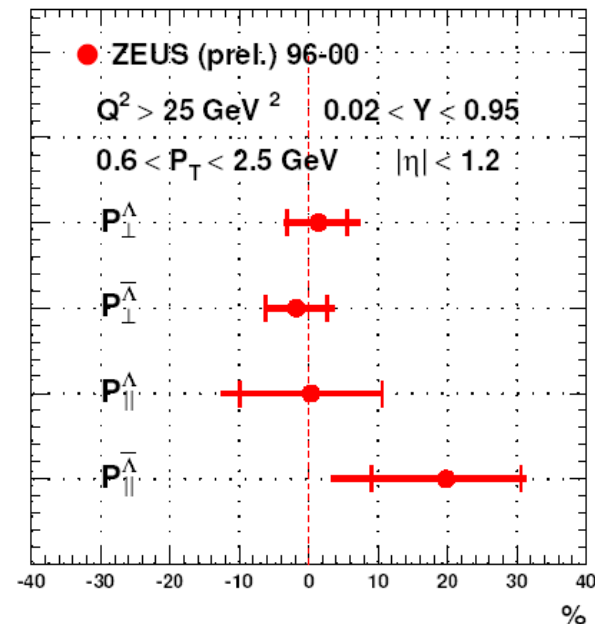
$\Lambda, \bar{\Lambda}$ polarisation

Angular distribution of $\Lambda \rightarrow \pi p$ decay in Λ rest-frame $(1 + \alpha P \cos \theta)$: $\alpha = 0.642$

ZEUS



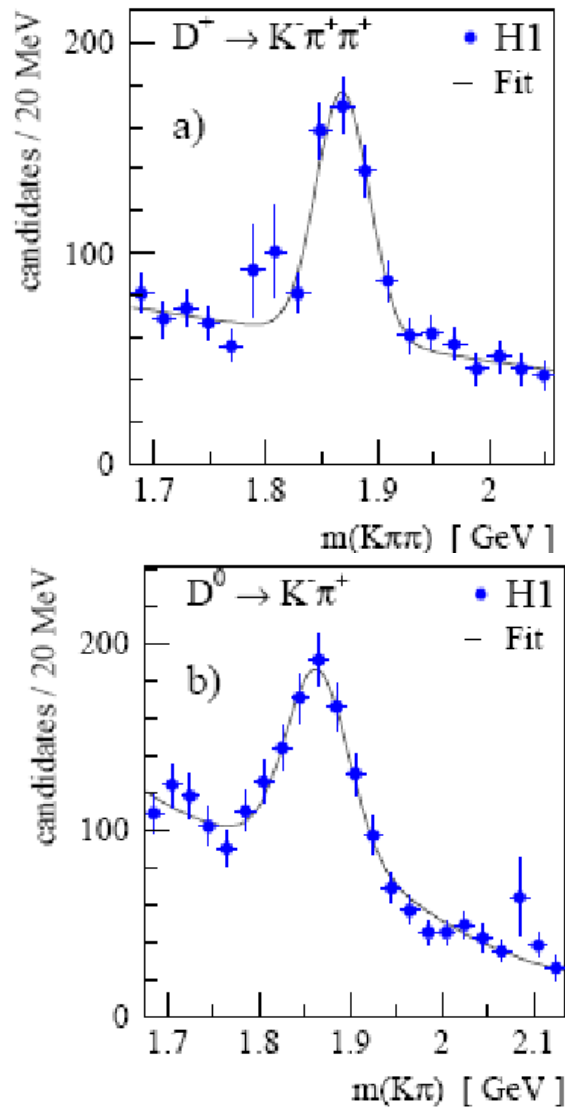
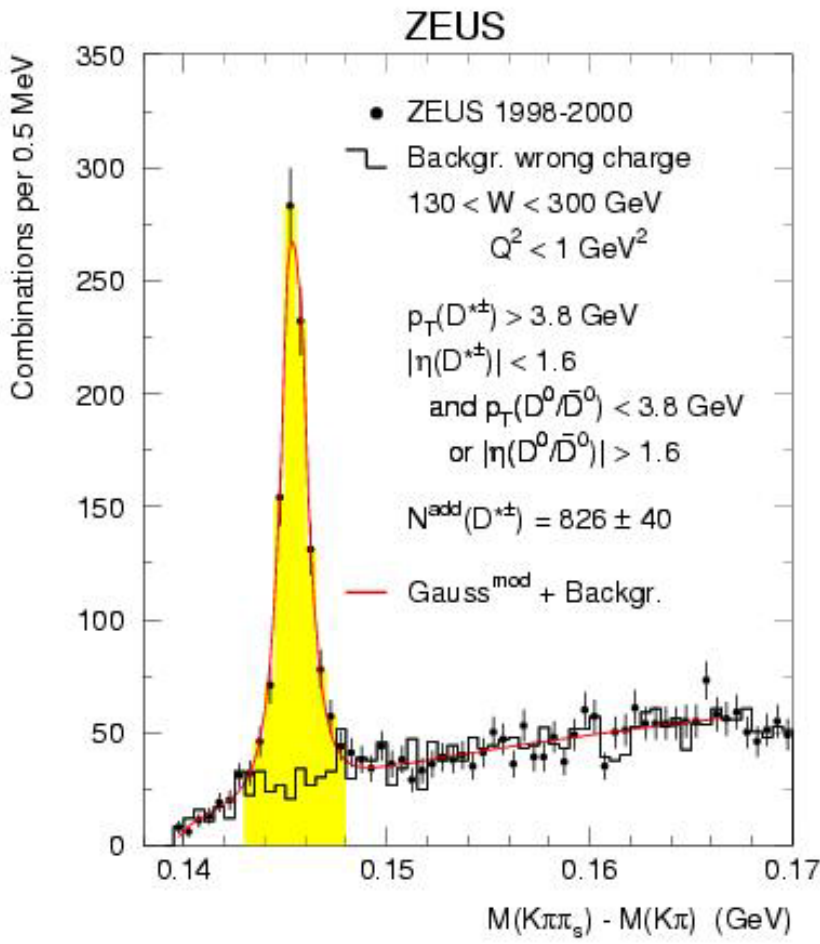
ZEUS



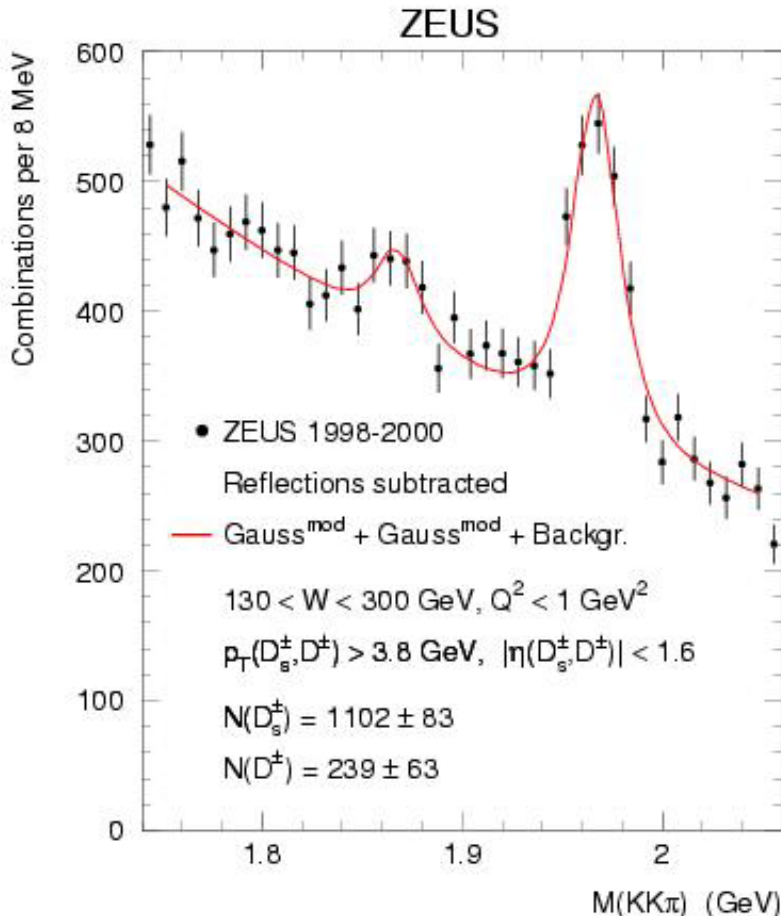
No $\Lambda, \bar{\Lambda}$ bar polzn with unpolarised e^\pm
?polarised beams at HERA-II

Charm production

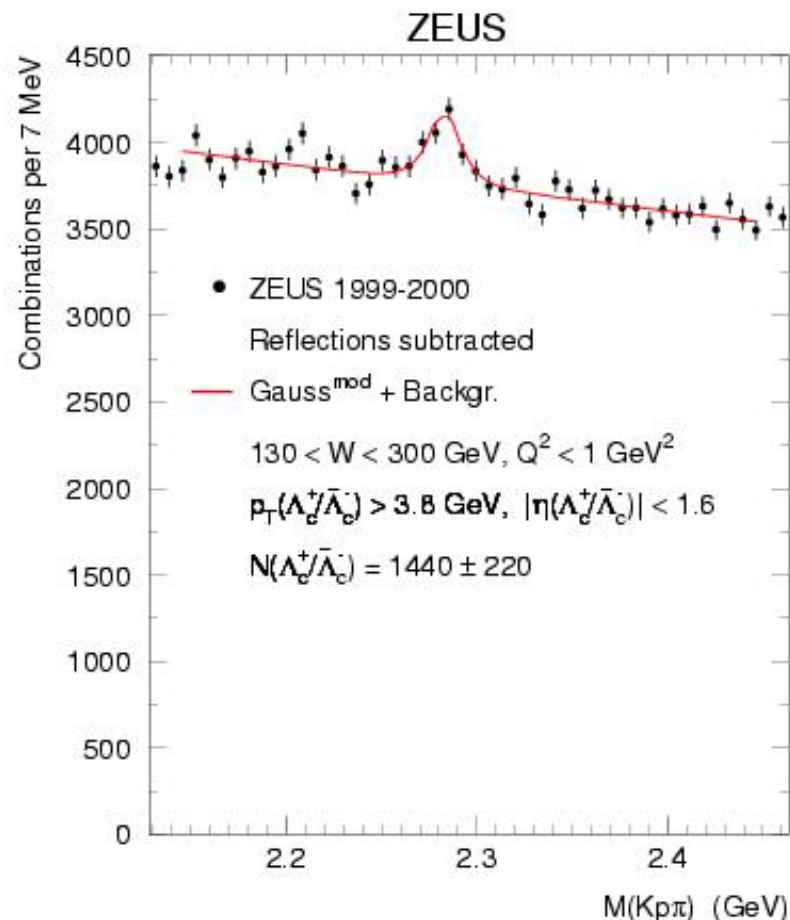
$D^{*+}, D^+, D^0, D_s^+, \Lambda_c^+$ observed



$D_s^\pm \rightarrow \phi\pi^\pm, \phi \rightarrow K^+K^-$: $\Lambda_c^+ \rightarrow pK^-\pi^+$ signals

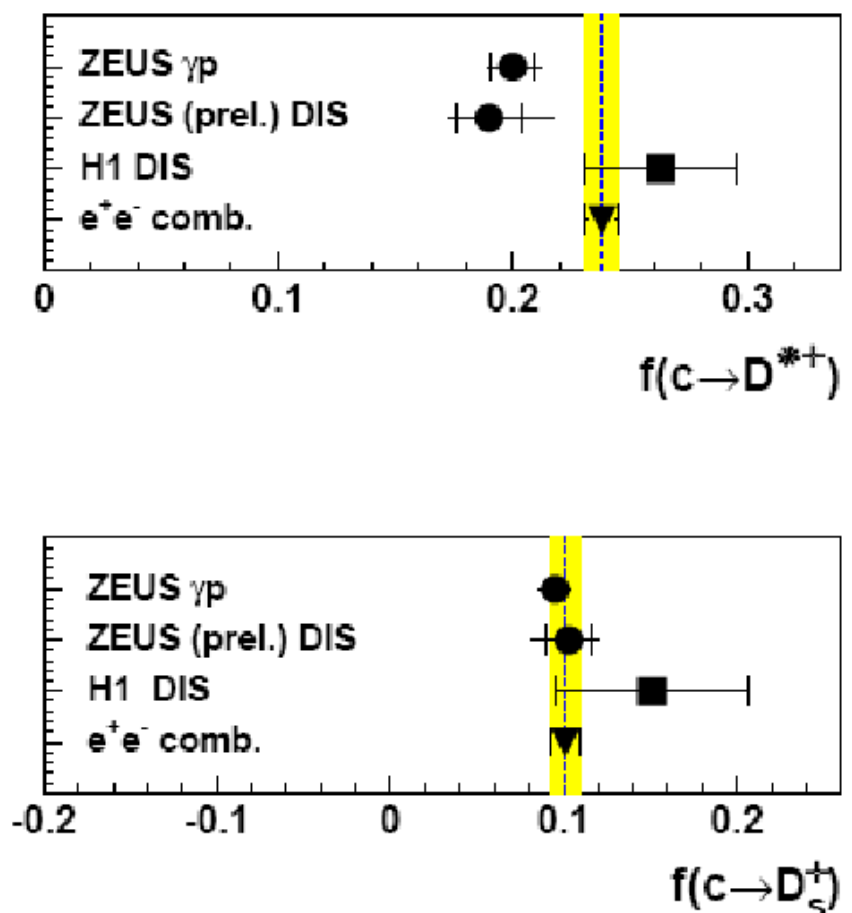
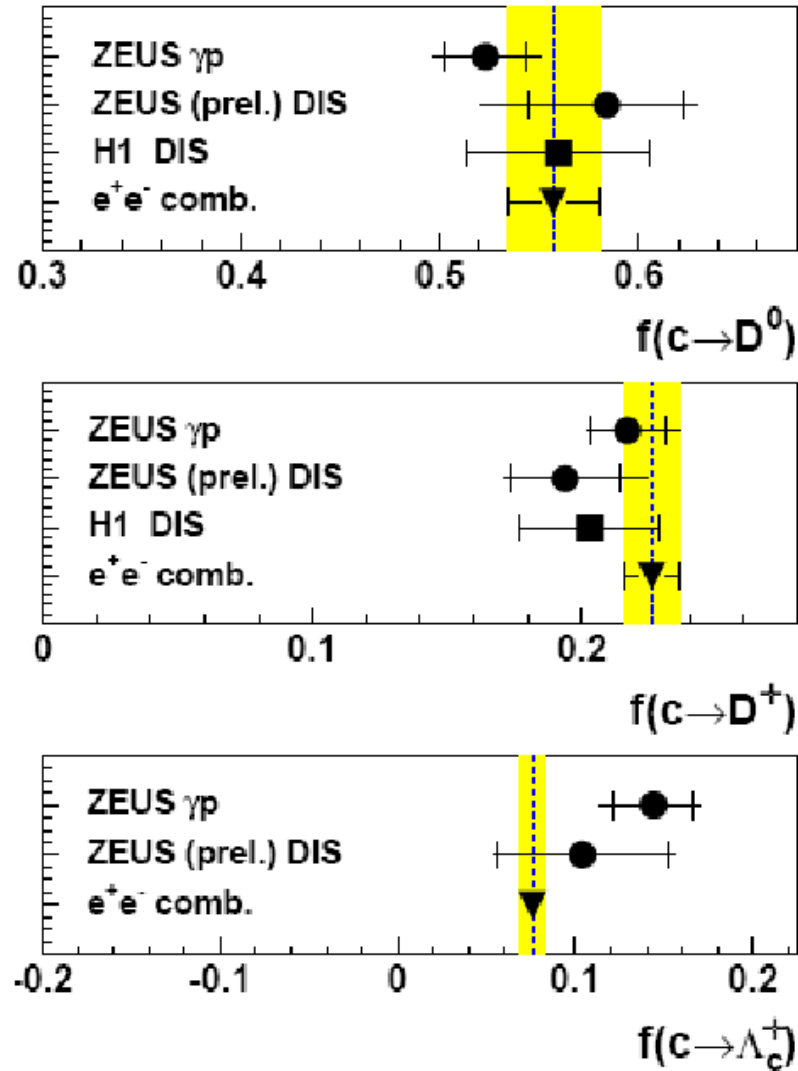


$M(KK)$ within 8 MeV of ϕ mass



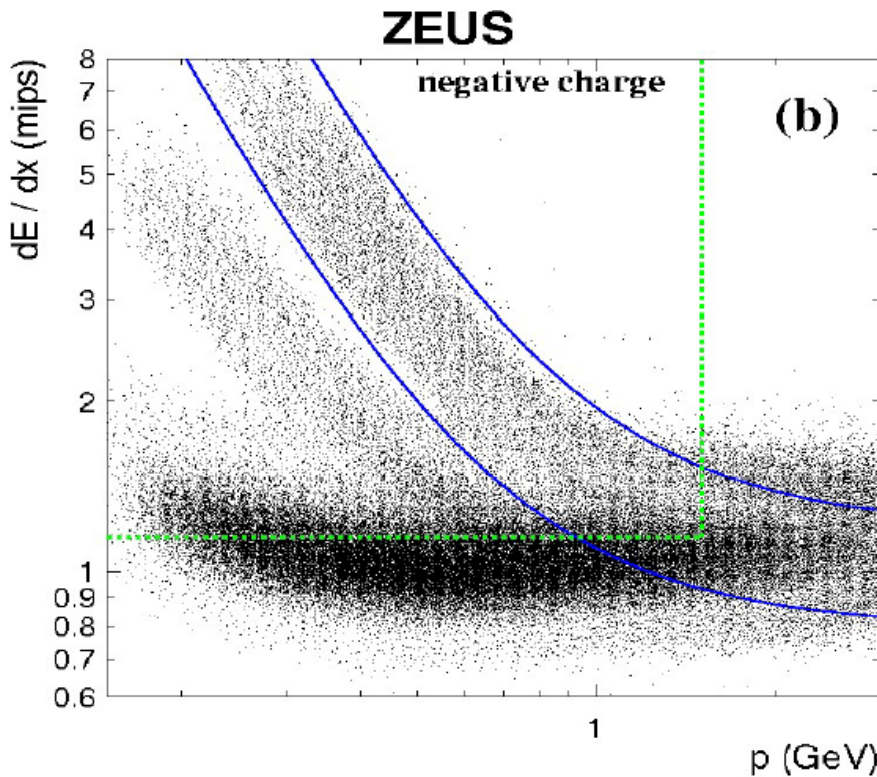
dE/dx info used for particle ID

Charm fragmentation supports universality



DIS, photoprod, e^+e^- annihilation
similar

Baryons decaying to strange particles



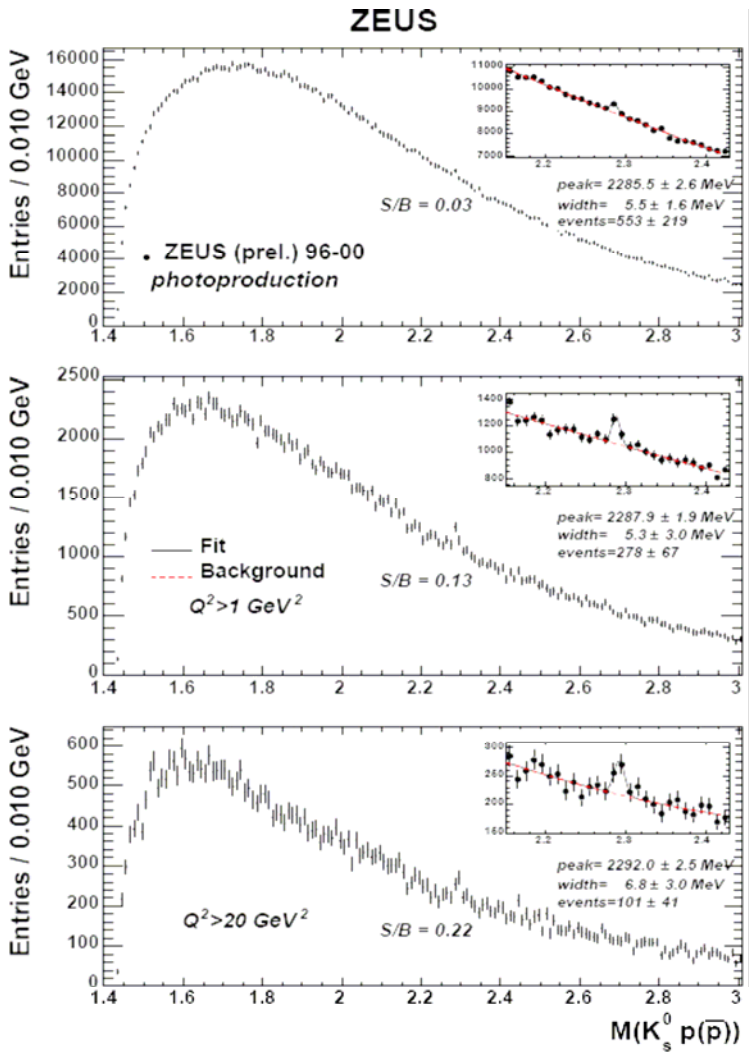
$K^0_s \rightarrow \pi^+ \pi^-$: secondary vertex.
 $p_T(K^0_s) > 0.3$ GeV, $|\eta(K^0_s)| < 1.5$
exclude Dalitz pairs, γ -conversions
exclude Λ candidates

p, \bar{p}, K^+, K^- reconstruction:
tracks from primary vertex
 dE/dx identification:
ZEUS – region method
in blue band
and $dE/dx > 1.5$ mips
and $p < 1.5$ GeV

H1 – likelihood method

$K^0_s p$ mass resolution
ZEUS 2.4, H1 5 MeV

$K^0_s p$ mass spectra ($\Lambda^*, \Sigma^*, \Lambda_c$, pentaquark)



Combinatorial backgrounds higher in γp ($\langle n_{ch} \rangle$ higher) & low Q^2

Mass peaks:

$\Theta^+(1520)$ candidate in DIS (see separate talk)

$\Lambda_c(2286)$ in PHP and DIS

seen equally in Kp , $Kp\bar{p}$

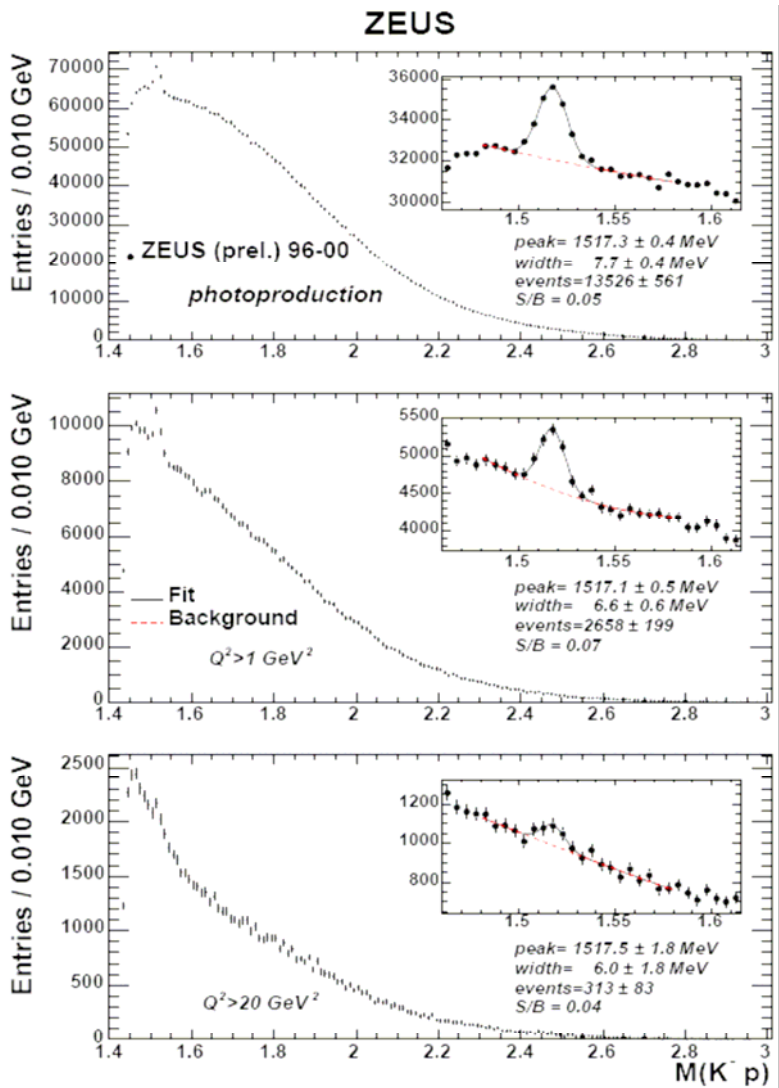
(162 ± 36 , 116 ± 38 ev)

seen equally $\eta > 0$, $\eta < 0$

(131 ± 40 , 145 ± 34 ev)

Consistent with $\gamma^* g \rightarrow c\bar{c}$

K^-p , K^+p^- mass spectra ($\Lambda(1520)$)

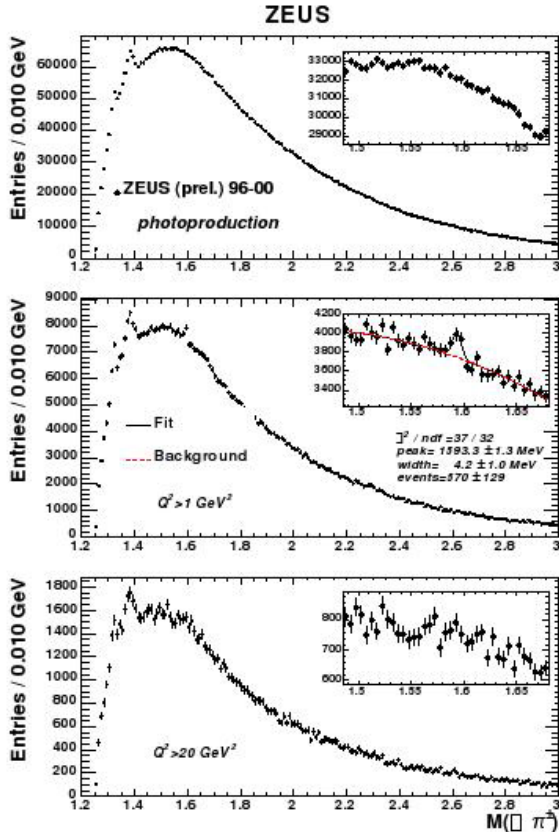


Mass peak:

$\Lambda(1520)$ in PHP and DIS
seen equally in Kp , $Kp\bar{}$
(1207 ± 143 , 1402 ± 142 ev)
seen equally $\eta > 0$, $\eta < 0$
(1337 ± 151 , 1246 ± 127 ev)

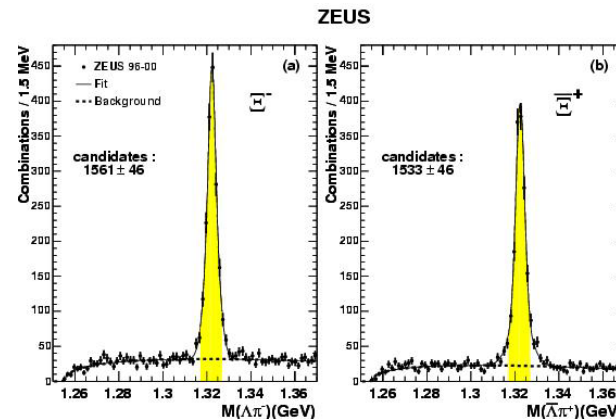
Consistent with $\gamma^* g \rightarrow q\bar{q}$

$\Lambda^0\pi^\pm$ mass spectra (Ξ, Σ^* , pentaquark)

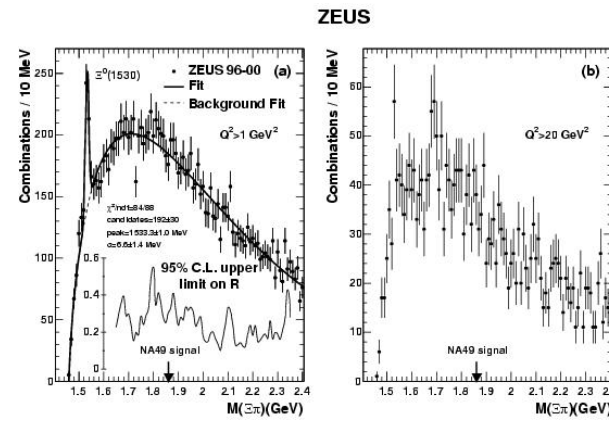


Observe: $\Xi(1320)$ $\Sigma^*(1385)$
No peak in $\Theta^+(1520)$ region

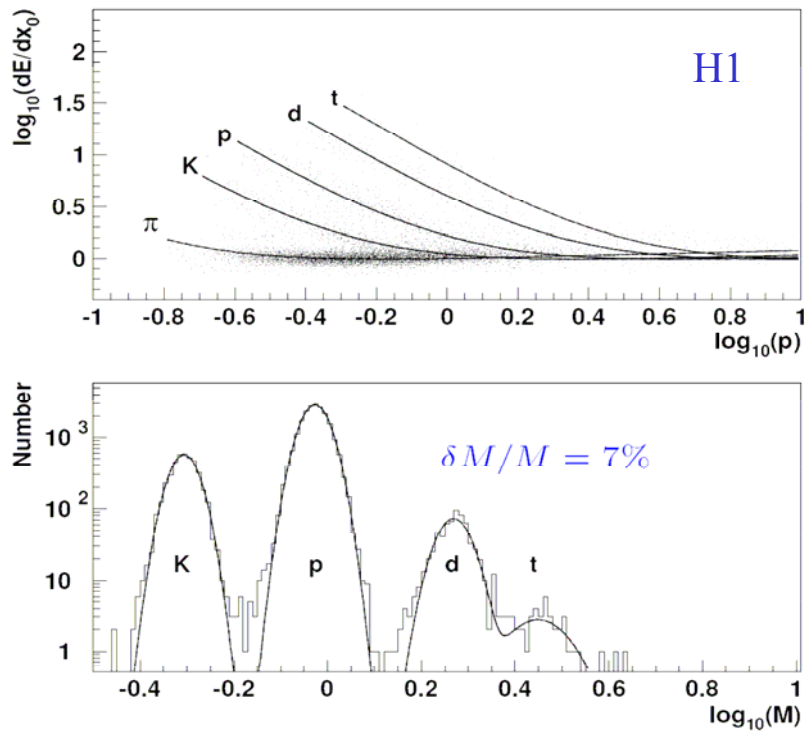
4.4 σ peak near 1600 MeV for
 $Q^2 > 1$ DIS: $\Sigma(1580)? \Sigma(1620)?$



Demand decay vtx: see $\Xi^- \rightarrow \Lambda\pi^-$, also $\Xi^* \rightarrow \Xi\pi$



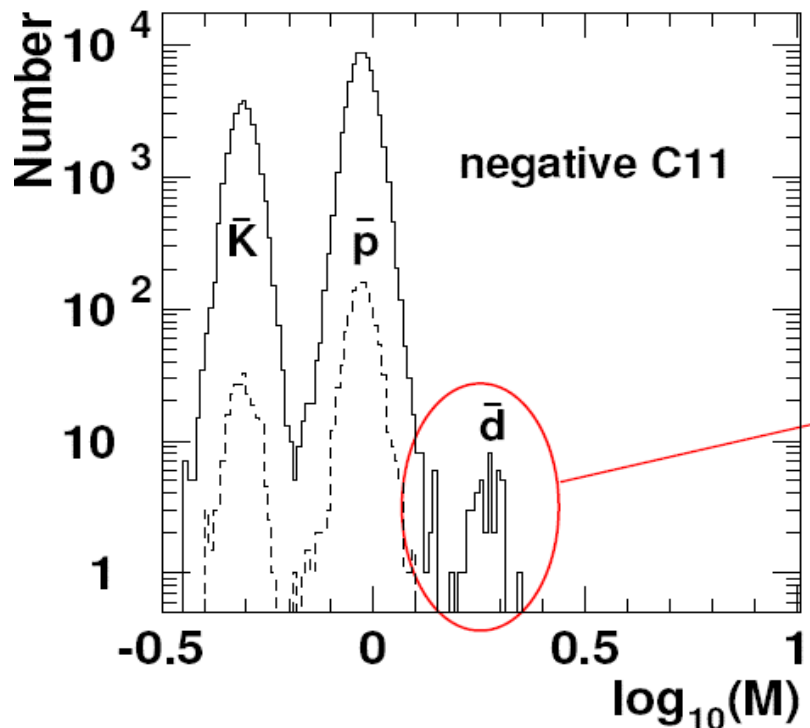
Anti-deuteron production and heavy particle search



d, t mainly from background

Nothing heavier than t seen.

$$\langle W_{\gamma,p} \rangle = 200 \text{ GeV}, \quad 0.2 < p_t/M < 0.7, \quad -0.4 < y_{\text{lab}} < 0.4$$

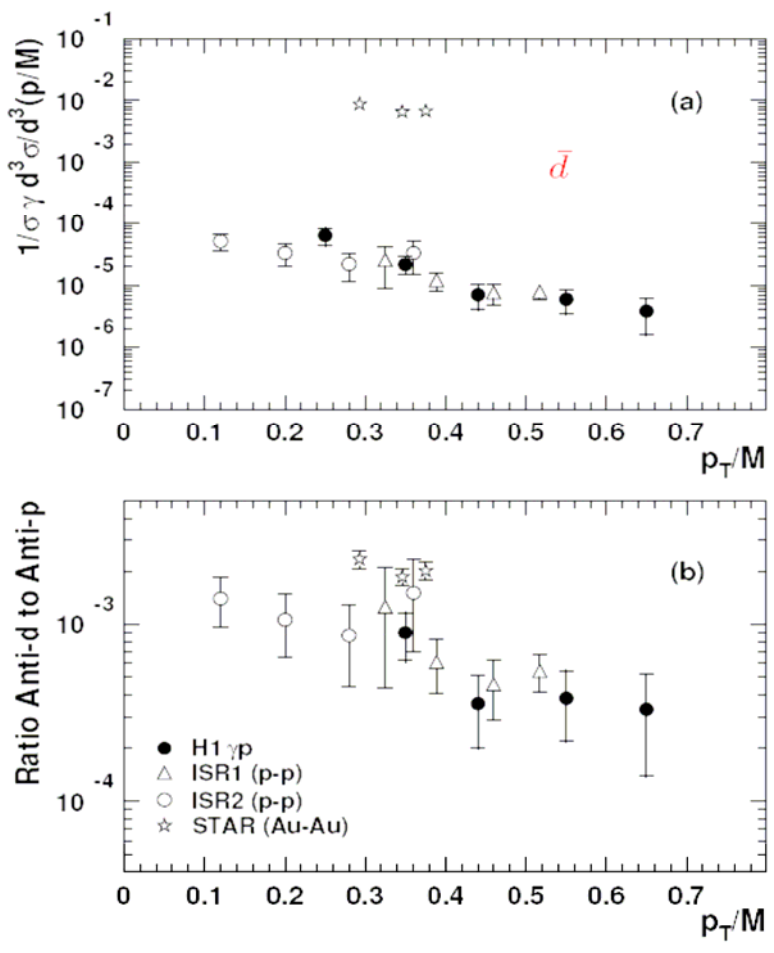


anti- d : physics beyond standard fragmentation

45 anti- d in 5.5 pb^{-1}

0 anti- t , 0 heavier

anti- d production: compare γp , pp , $AuAu$



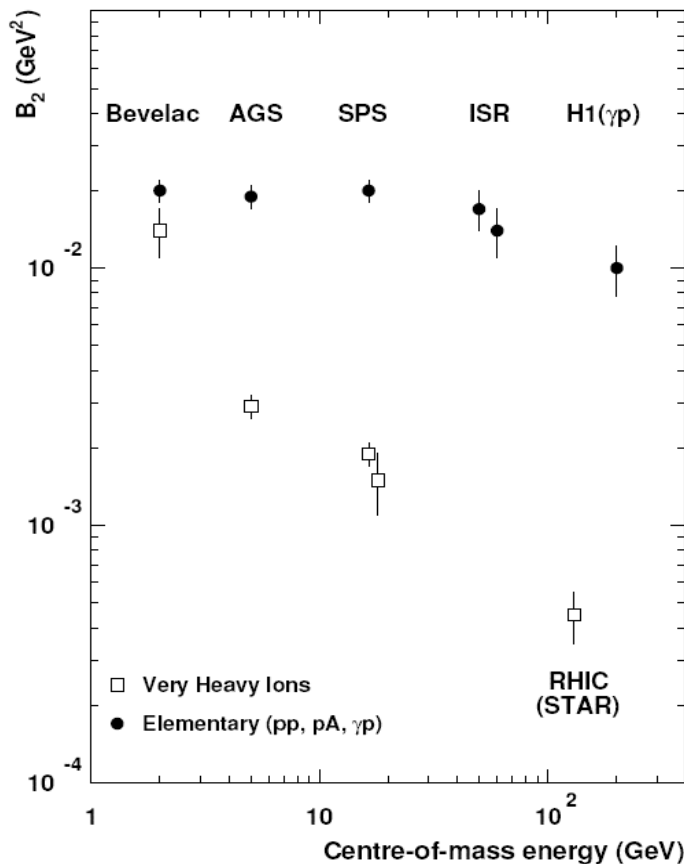
$\sigma(\bar{d}) = 2.7 \pm 0.5 \pm 0.2 \text{ nb}$
 $\sigma(M_{-\bar{d}/+} > M_{\bar{d}/t}) < 0.19 \text{ nb} @ 95\% \text{ C.L.}$
 $0.2 < p_t/M < 0.7, |y_{lab}| < 0.4$

Normalised invariant cross-sections:

$\gamma p, pp$ good agreement
 $AuAu$ much higher

\bar{d}/p ratio higher in $AuAu$ also

anti-*d* production: compare γp , pp , $AuAu$



Coalescence model:

$$\frac{1}{\sigma} \frac{d^3 \sigma(d)}{d^3 p} = B_2 \left(\frac{1}{\sigma} \frac{d^3 \sigma(p)}{d^3 p} \right) \left(\frac{1}{\sigma} \frac{d^3 \sigma(n)}{d^3 p} \right)$$

B_2 inversely proportional to size of interaction region.

γp : $B_2 = 0.010 \pm 0.002 \pm 0.001$

Similar values in pp , pA

Much lower values in $AuAu$

(Very heavy ions):

Bevalac ($NeAu$), AGS ($AuPt$), SPS($PbPb$)

Bose-Einstein correlations: $K_s^0 K_s^0$ and $K^\pm K^\pm$

ZEUS

Study space-time structure of particle source via, $f(Q_{12})$, its Fourier transform

Earlier shown BEC independent of Q^2

Correlation function: $R(p_1, p_2) = \rho(p_1, p_2)/\rho(p_1)\rho(p_2) = |1 + f(Q_{12})|^2$
where $Q_{12} = p_1 - p_2$

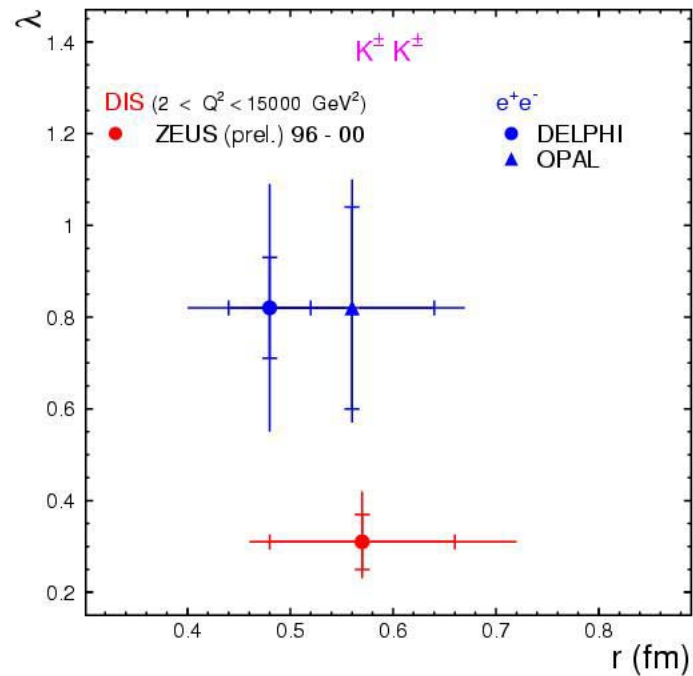
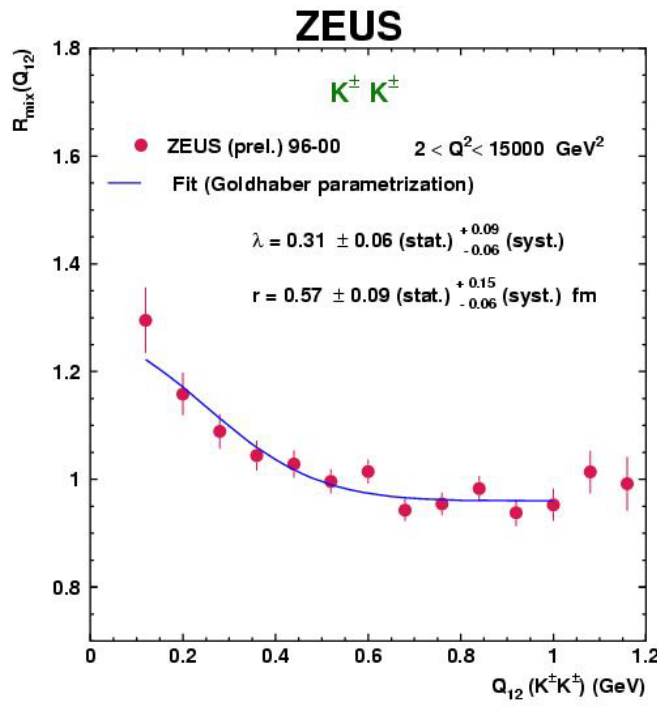
Fit function: $R(Q_{12}) = \alpha(1 + \delta Q_{12})(1 + \lambda \exp[-r^2 Q_{12}^2])$
 r = source radius, $0 < \lambda < 1$

Measure $R(Q_{12})$ in data by event-mixing double ratio

$$R = \{P(\text{data})/P_{\text{mix}}(\text{data})\} / \{P(\text{MC})/P_{\text{mix}}(\text{MC})\}$$

All evaluated at the same Q_{12} . MC has no BE correlations

Bose-Einstein correlations: $K^\pm K^\pm$



r -value similar to charged pions

$$\pi^\pm \pi^\pm: r = 0.666 \pm 0.009 {}^{+0.022}_{-0.036}$$

$$K^\pm K^\pm: r = 0.57 \pm 0.09 {}^{+0.015}_{-0.06}$$

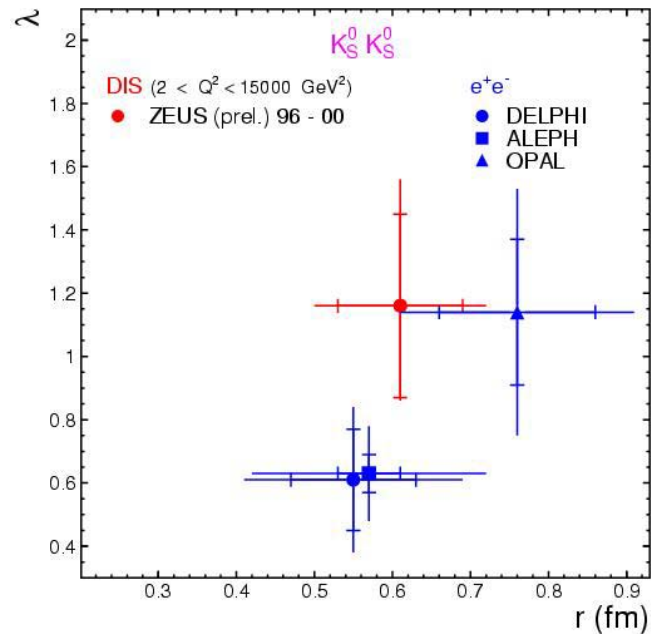
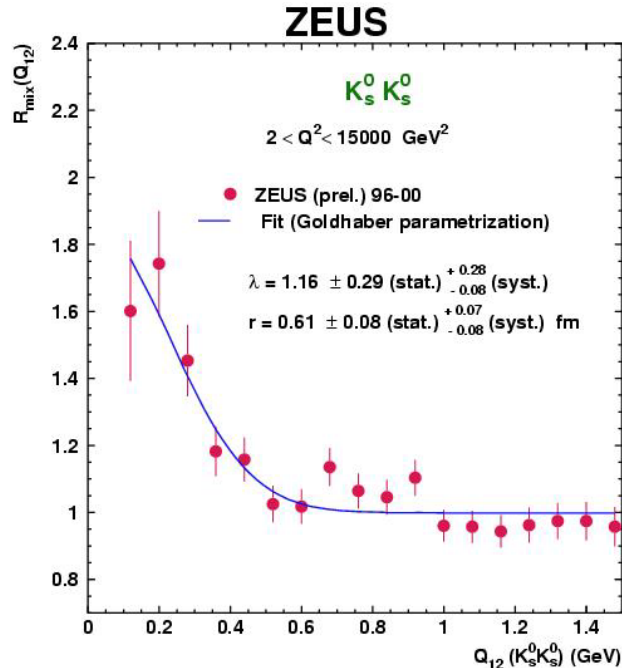
r -value agrees with LEP

λ -value is lower. Reasons:

?different fragmentation,

? $\phi^0(1020)$ decay in p -fragmentation region

Bose-Einstein correlations: $K_s^0 K_s^0$



LEP: clear hierarchy $r(\pi^\pm) > r(K^\pm) > r(\Lambda)$

ZEUS: $r(\pi^\pm) \sim r(K^\pm) \sim r(K_s^0)$

$\pi^\pm \pi^\pm$: $r = 0.666 \pm 0.009^{+0.022}_{-0.036} \text{ fm}$

$K^\pm K^\pm$: $r = 0.57 \pm 0.09^{+0.15}_{-0.06} \text{ fm}$

$K_s^0 K_s^0$: $r = 0.61 \pm 0.08^{+0.07}_{-0.08} \text{ fm}$

$r \text{ (DIS)} \sim r \text{ (LEP)}$

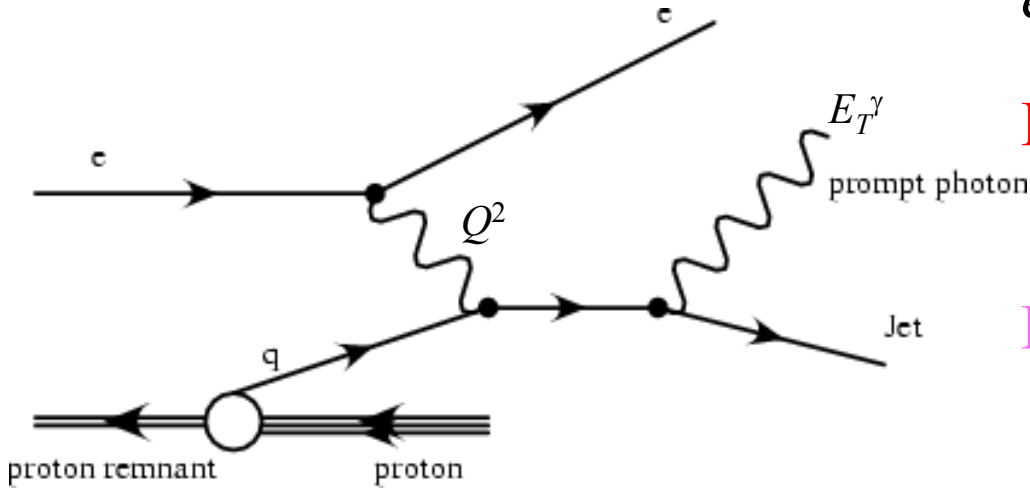
$\lambda \text{ (DIS)} > \lambda \text{ (LEP)}$

reasons: ? $f_0(980) \rightarrow K_s^0 K_s^0$

affects λ at low Q_{12}

(ALEPH,DELPHI removed $f_0(980)$ effects)

Prompt photon production: γ radiation from quark line



$$eq \rightarrow eq\gamma$$

DIS: isolated e, γ (incl.)
isolated e, γ, jet

Photoprod'n ($Q^2 < 1 \text{ GeV}^2$)
 e unobserved
isolated γ ,
jet balancing p_T

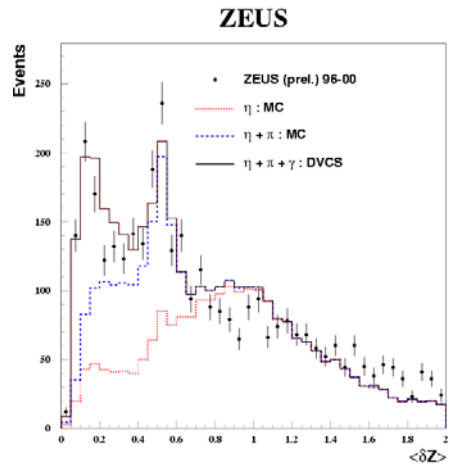
Backgrounds: γ radiation from initial state, final state e (DIS)
 γ from jet fragmentation
 γ from π^0, η^0 decay

γ signal – π^0 and η^0 backgrounds

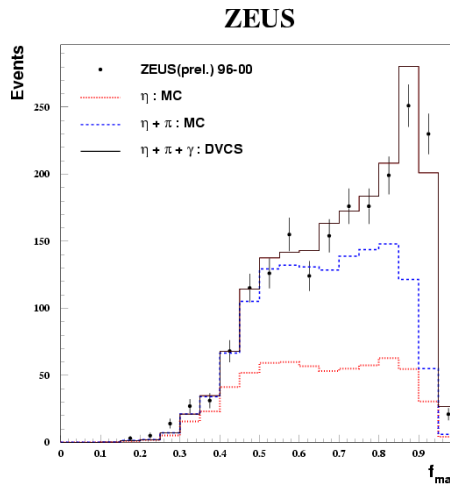
Use e.m. calorimeter shower shape

ZEUS
DIS

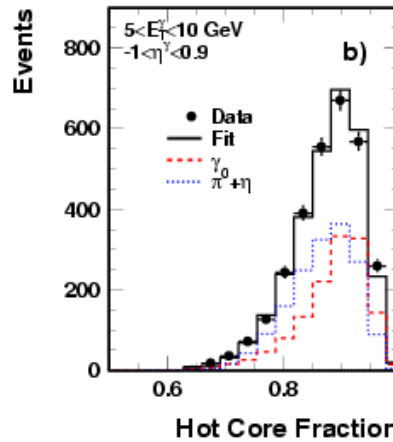
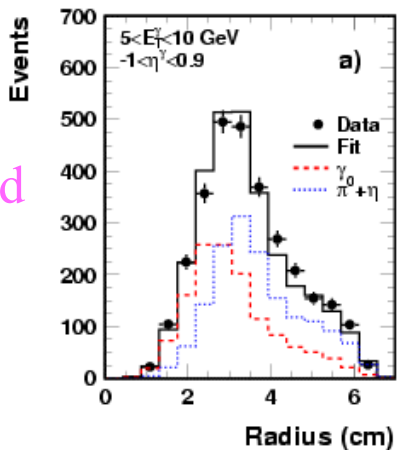
Shower width



Hot core fraction



H1
photoprod



ZEUS z-strips

γ shape from DVCS data
 π^0, η^0 shapes from MC
Fit for γ, π^0, η^0 fractions

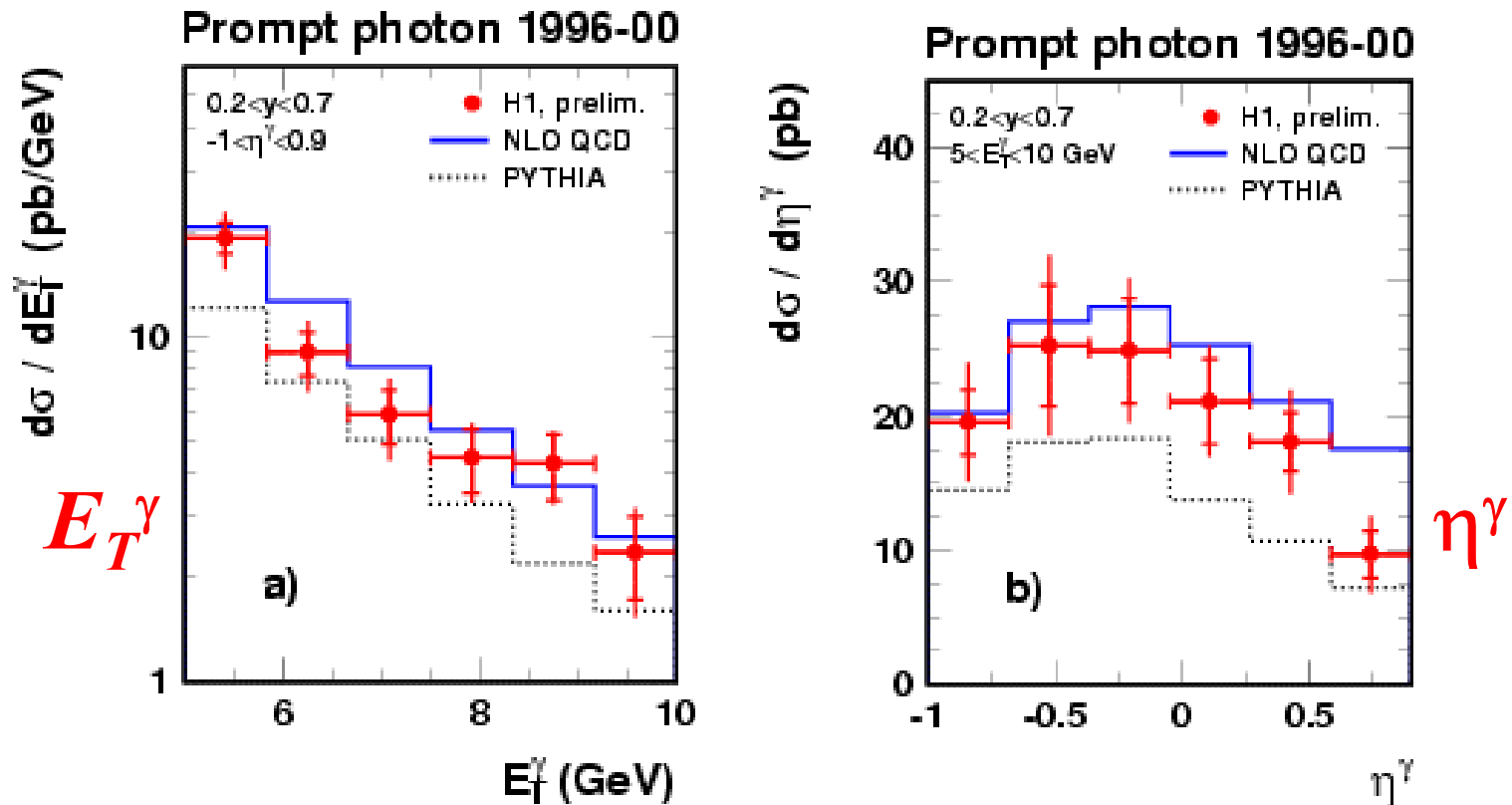
Background subtraction is
rather stable against errors
in γ shape.

H1 cells

$\gamma, (\pi^0 + \eta^0)$ shapes from MC
Likelihood discriminator
in (E_T, η) bins

Photoproduction:

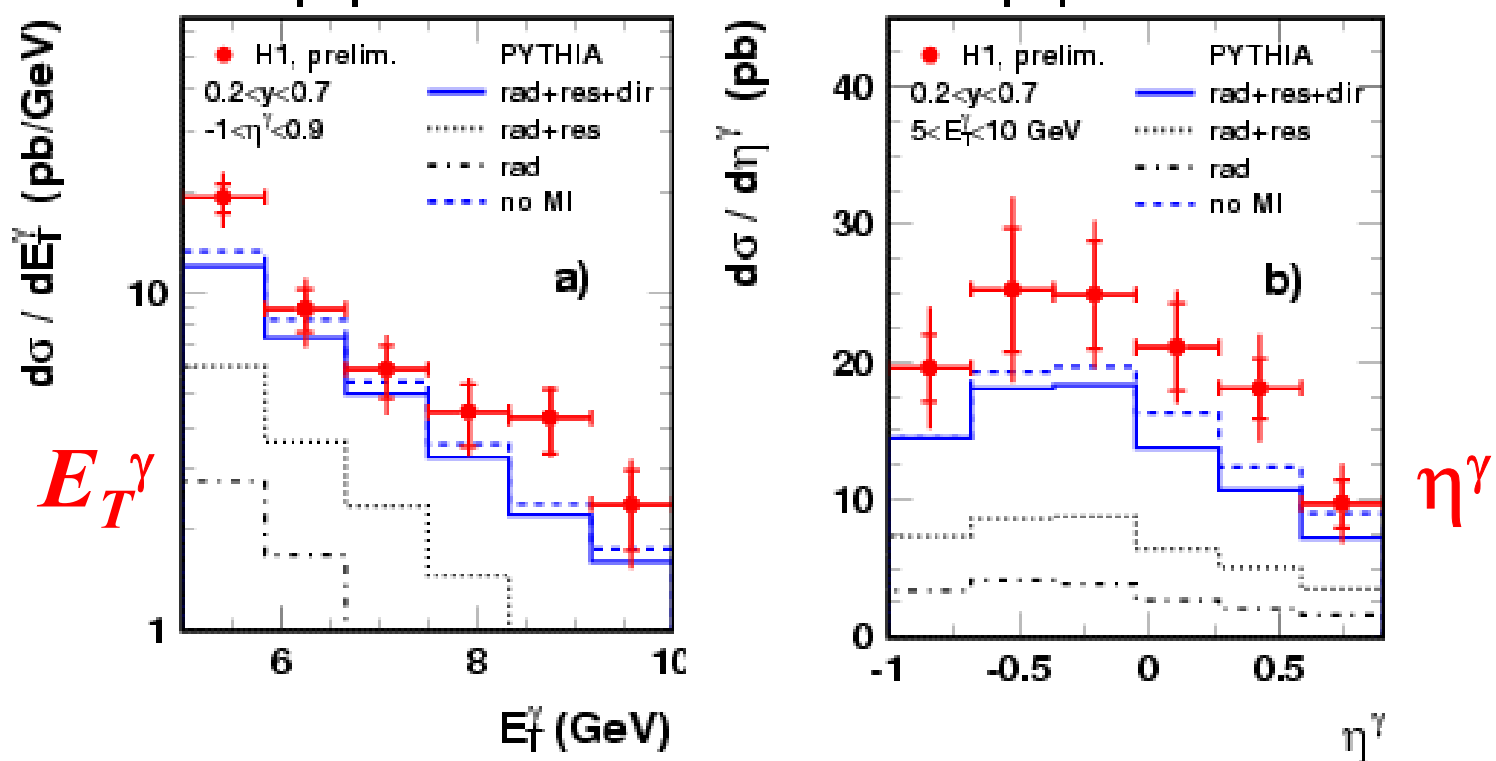
H1: compare to NLO and PYTHIA



pQCD (NLO, Fontannaz *et al*) agrees within errors
PYTHIA: describes shapes but a bit low.

Photoproduction:

PYTHIA – origin of prompt γ

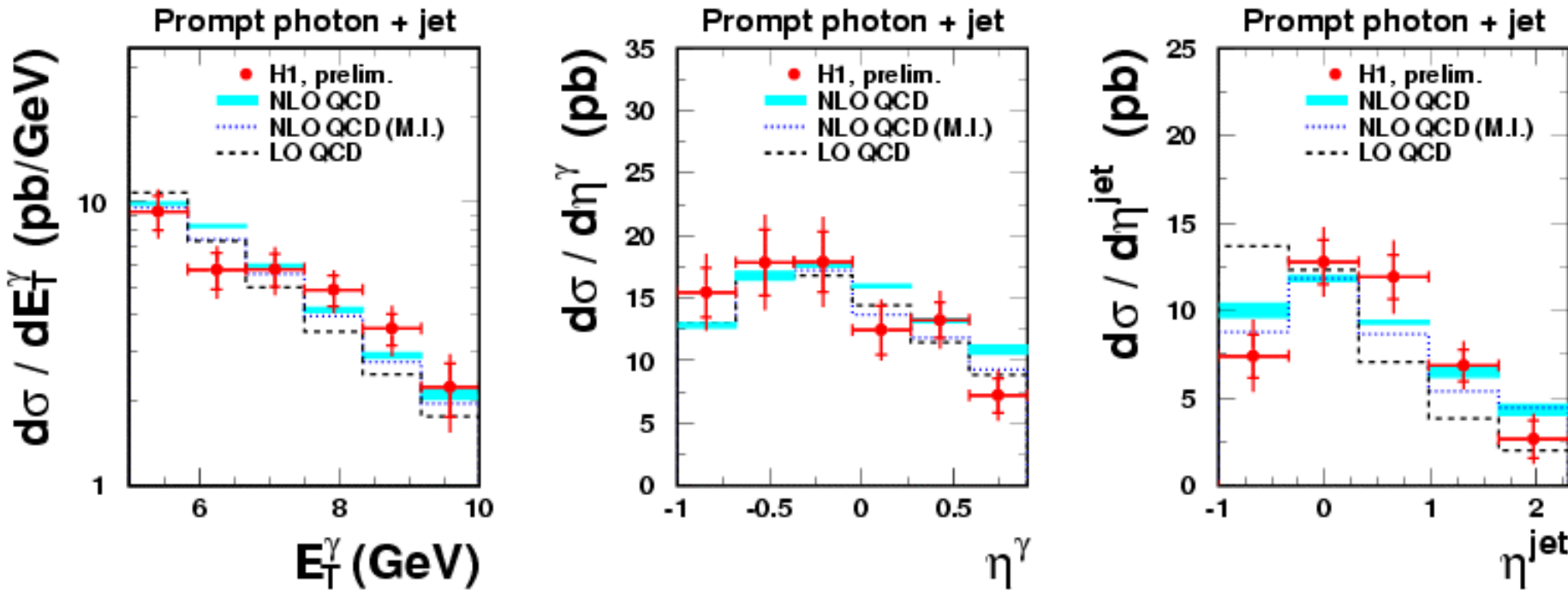


- >50% direct exchanged γ .
- Radiation from electron line small
- Multiple interactions hurt photon isolation cut and so reduce the cross-section

Photoproduction:

$\gamma + \text{jet} - \text{compare to LO and NLO}$ (Fontannaz *et al*)

(NLO scale variation 0.5 E_T^γ to 2 E_T^γ)



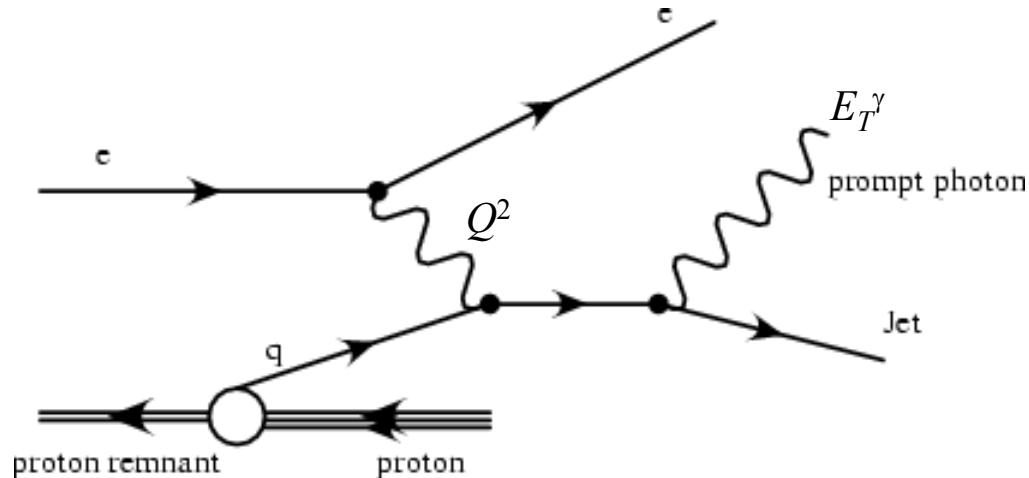
Correction to NLO for multiple interactions applied by PYTHIA

– improves fit at large η^γ

Large negative NLO corrections at $\eta_{\text{jet}}^{\text{jet}} < 0$

NLO describes the data within errors

$eq \rightarrow eq\gamma$ in Deep Inelastic Scattering



Minimise ISR, FSR

$(139.8^\circ < \theta_e < 171.9^\circ)$ far from γ

Two hard scales:

(Q^2, E_T^γ) hard for MC to simulate
PYTHIA v6.206 (new)
HERWIG v6.1

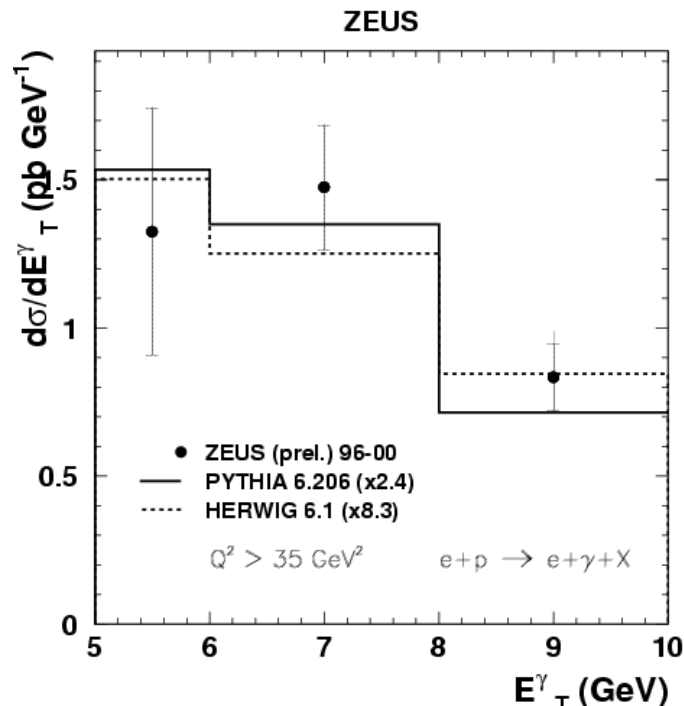
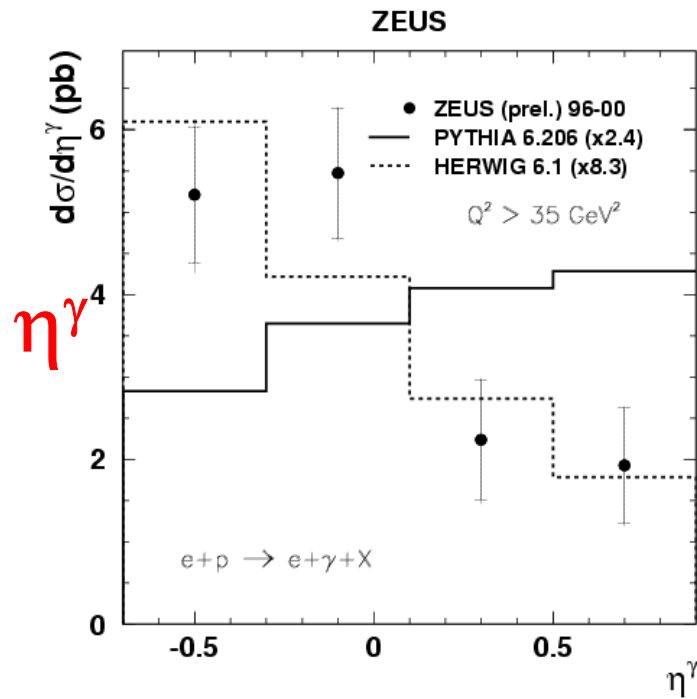
Comparisons available for $e\gamma X$, $e\gamma$ jet

NLO calculations $O(\alpha^3\alpha_s)$ by Kramer and Spiesberger

Based on A. Gehrmann-de Ridder,K,S Nucl. Phys. **B578** (2000) 326

- includes ISR, FSR, vertex diagrams, all interferences,
- predictions for ($e+\gamma+one\ jet$) including renorm. scale uncertainty

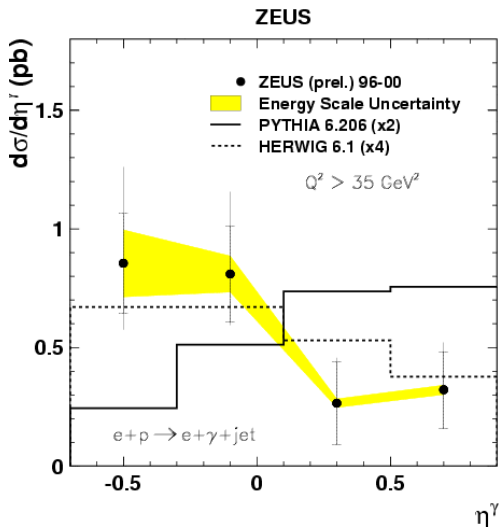
DIS: $eq \rightarrow e\gamma X$ (inclusive)



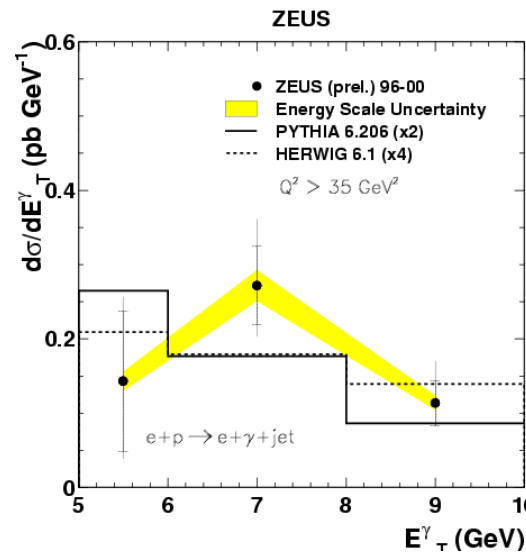
	$\langle Q^2 \rangle (\text{GeV}^2)$	$\langle x_{Bj} \rangle$	η^γ shape	$E_{T\gamma}$ shape	normalisation factor needed
Data	87	0.0049			
PYTHIA	87	0.0047	BAD	OK	2.4
HERWIG	62	0.0017	OK	OK	8.3

NEITHER IS A GOOD DESCRIPTION OF THE DATA.

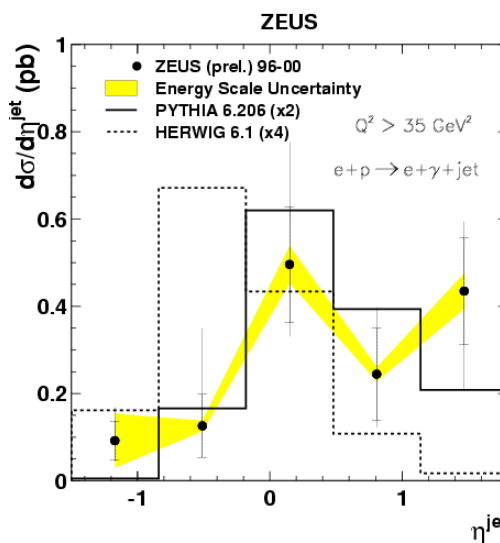
DIS: $eq \rightarrow e\gamma + \text{one jet}$



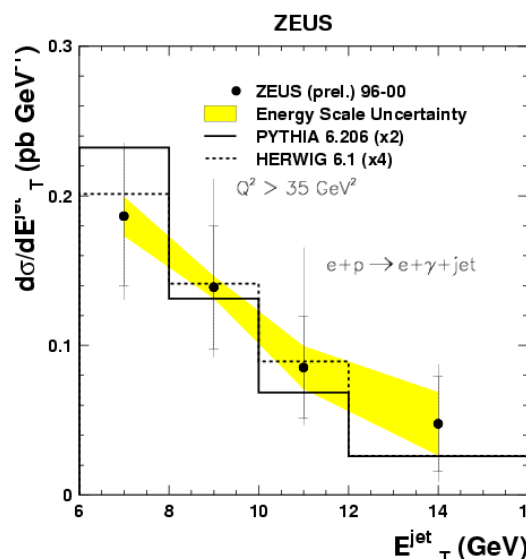
η^γ
HERWIG
preferred



E_T^γ
Data uneven.
MC's similar



η^jet
PYTHIA
preferred



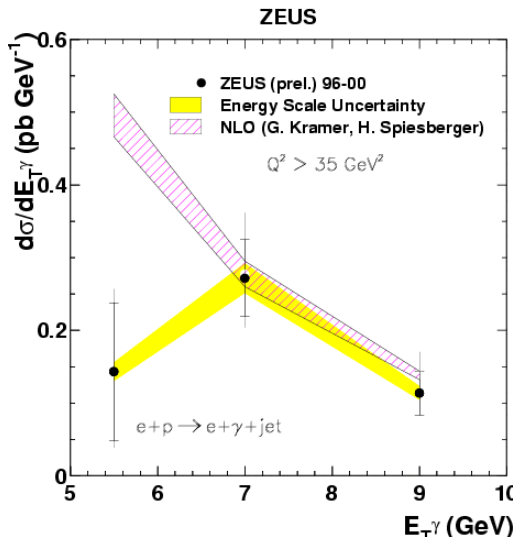
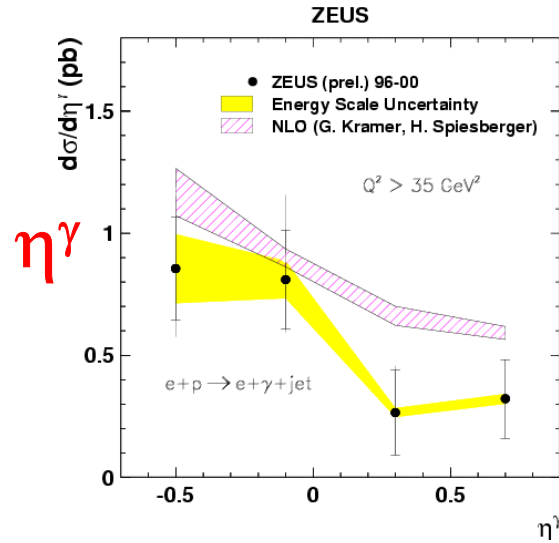
E_T^jet
OK

Normalisation:
Both poor

DIS: $eq \rightarrow e\gamma + \text{one jet}$

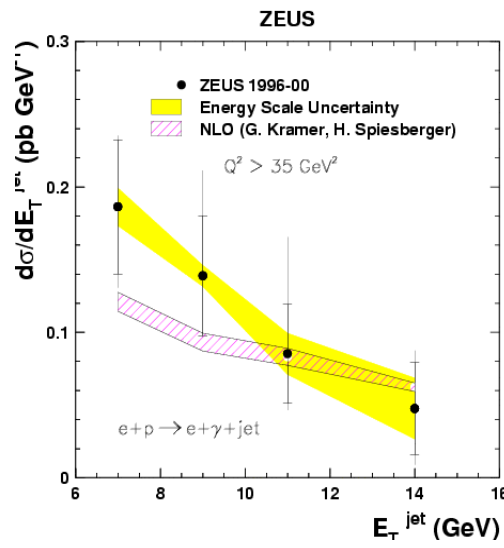
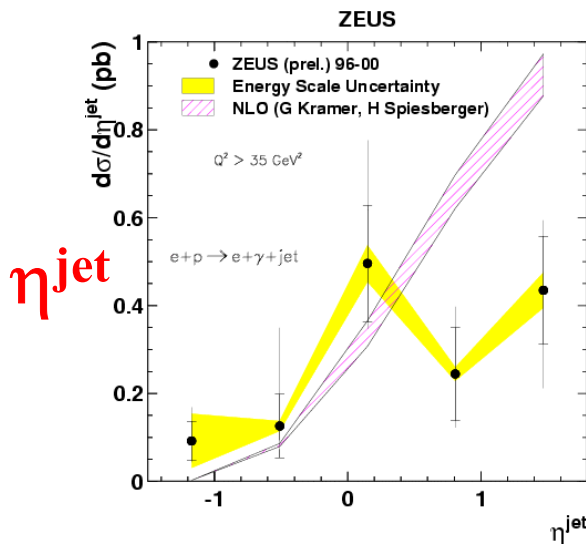
Comparison to NLO calculations

(Kramer & Spiesberger)



$E_T\gamma$

Total cross section:
Data slightly below theory
(1.7 S.D.)

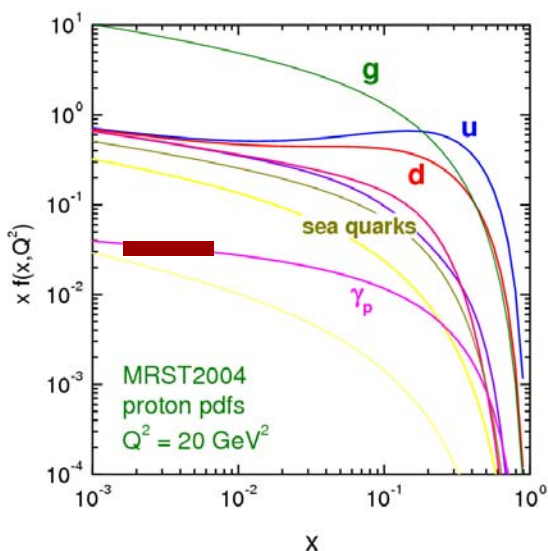
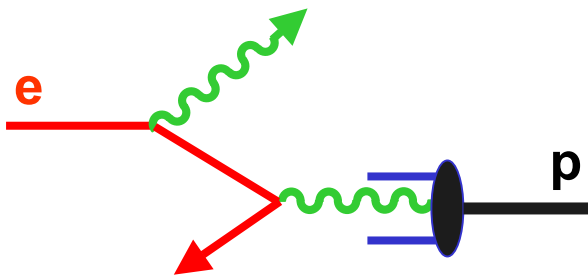


E_T^{jet}

Overall: ‘fair’ agreement
rates well predicted

MRST:

first measurement of $\gamma_p(x, Q^2)$?



ZEUS: “Observation of high E_T photons in deep inelastic scattering”, hep-ex/0402019

$\sqrt{s} = 318 \text{ GeV}$, $Q^2 > 35 \text{ GeV}^2$, $E_e > 10 \text{ GeV}$

$139.8^\circ < \theta_e < 171.8^\circ$

$5 < E_{T\gamma} < 10 \text{ GeV}$, $-0.7 < \eta_\gamma < 0.9$

$\sigma(ep \rightarrow e\gamma X) = 5.64 \pm 0.58 \text{ (stat.)} \pm \frac{0.47}{0.72} \text{ (syst.) pb}$

prediction using MRST2004 QEDpdfs:

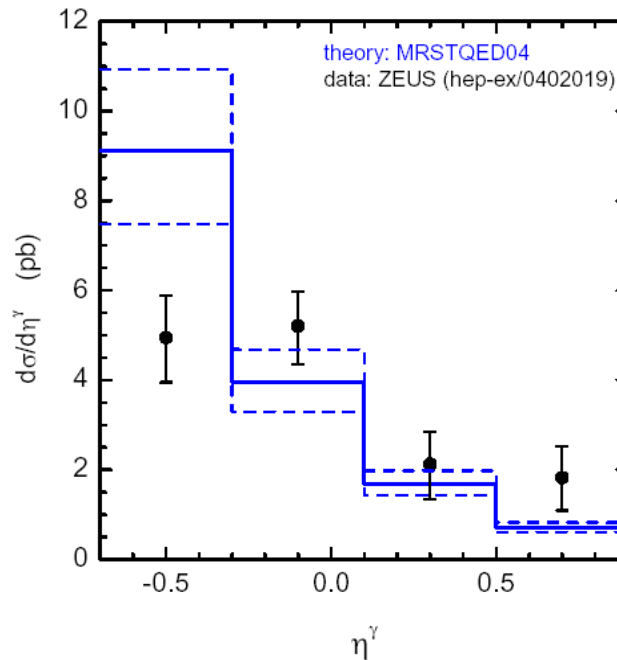
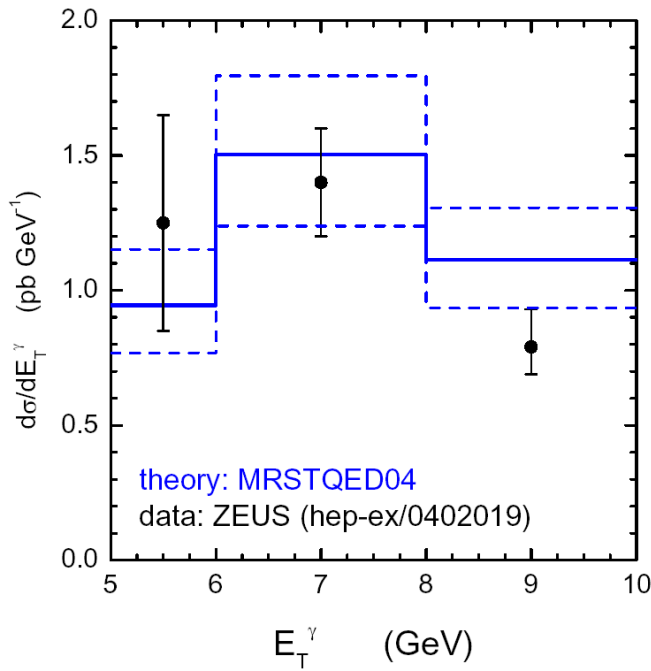
$\sigma(ep \rightarrow e\gamma X) = 6.2 \pm 1.2 \text{ pb (scale dependence)}$

Note: exchanged e^* carries the Q^2

MRST: lowest order theory. No jets prediction. $p_t(e) = p_t(\gamma)$

$$e \gamma_p(x, Q^2) \rightarrow e \gamma$$

Absolute rate prediction



$\langle Q^2 \rangle = 75$ (cf data 87). Would increase with higher orders

Encouraging agreement. Can they predict ($\gamma + \text{jets}$) distributions?

Summary

Charged Multiplicities in DIS and DDIS

use of $W, E_{current}$: unified look at DIS, DDIS

Inclusive photoproduction of non-strange mesons

universal rate as function of $(p_T + m)$

Strange Particle production

$p_T, \eta, Q^2, x, \Lambda$ polarisation

Charm fragmentation

universality: DIS, photoproduction, e^+e^-

Baryons decaying to strange particles

dE/dx for K^\pm, p : resonances seen, pentaquark search

Antideuteron production

dE/dx . Coalescence model

KK Bose-Einstein correlations

compare LEP, $f_0(980)$ issues

Prompt photon production in DIS

first measurement of $\gamma p(x, Q^2)$?

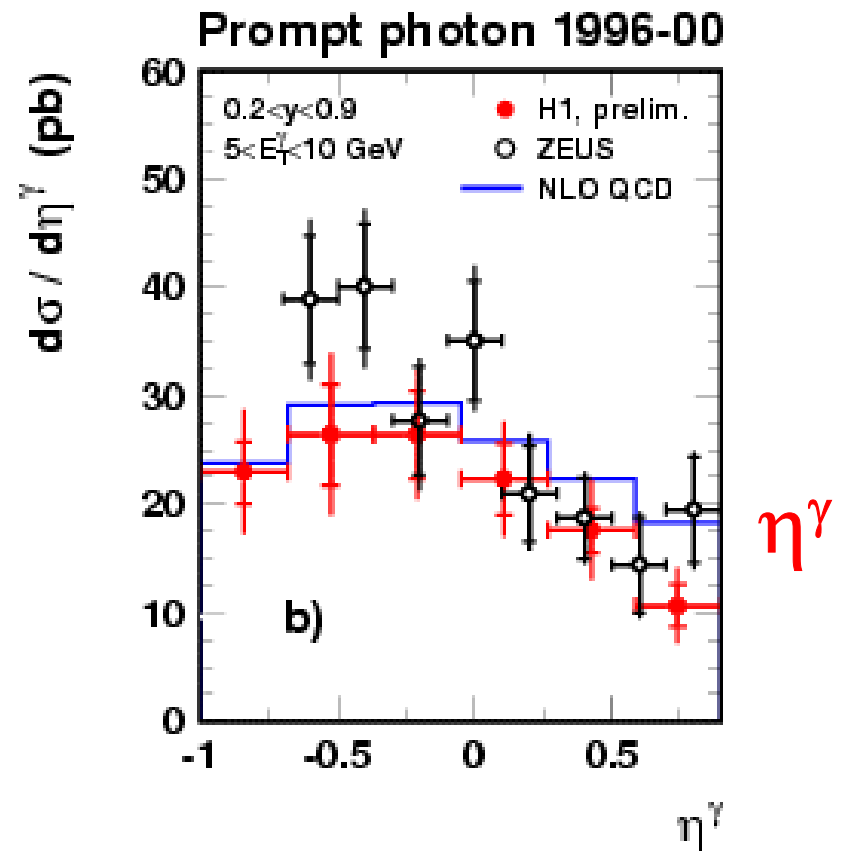
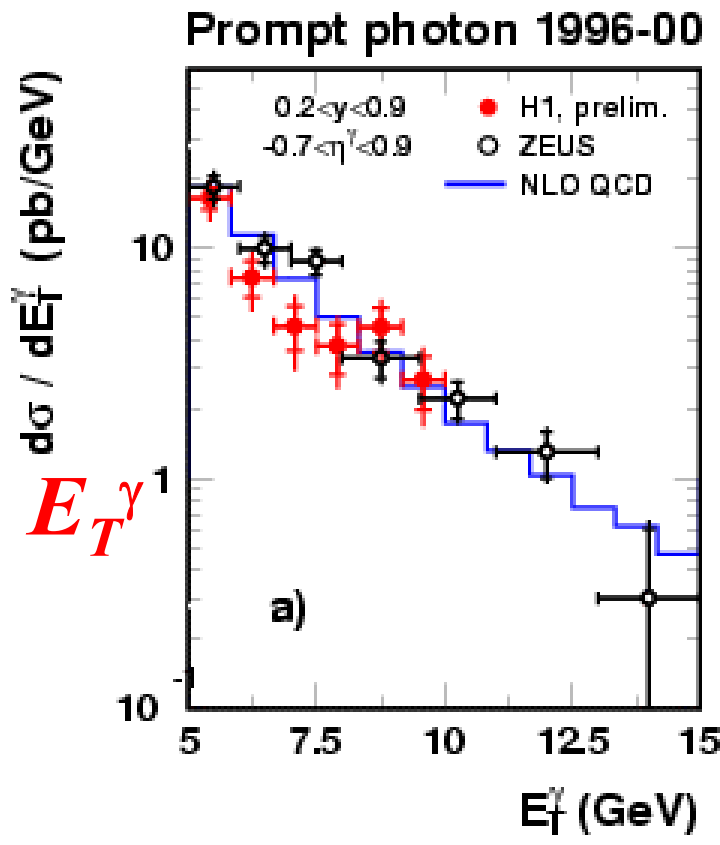
Kinematic region

H1 photoproduction	ZEUS photoprod'n (old)	ZEUS DIS
96-00 data (105 pb^{-1})	96-97 data (38 pb^{-1})	96-00 data (121 pb^{-1})
$Q^2 < 1 \text{ GeV}^2$		$Q^2 > 35 \text{ GeV}^2$
$5 < E_T^\gamma < 10 \text{ GeV}$ (15 GeV for ZEUS photo $d\sigma/d E_T^\gamma$)		
$-1.0 < \eta^\gamma < 0.9$	$-0.7 < \eta^\gamma < 0.9$	
$122 < W < 266 \text{ GeV}$	$134 < W < 285 \text{ GeV}$	$31(69)\% @ 300(318) \text{ GeV}$
Isolation: $E_t^\gamma / E_t^{\text{total}} > 0.9$ in cone of $\Delta R = (\Delta\Phi^2 + \Delta\eta^2)^{1/2} = 1$		
Prompt photon + jet		
Inclusive k_T	Cone $\Delta R = 0.7$	
$E_t^{\text{jet}} > 4.5 \text{ GeV}$	$E_t^{\text{jet}} > 5 \text{ GeV}$	$E_t^{\text{jet}} > 6 \text{ GeV}$
$-1.0 < \eta^{\text{jet}} < 2.3$	$-1.5 < \eta^{\text{jet}} < 1.8$	

Table after Lemrani

Photoproduction:

Inclusive prompt photon cross section

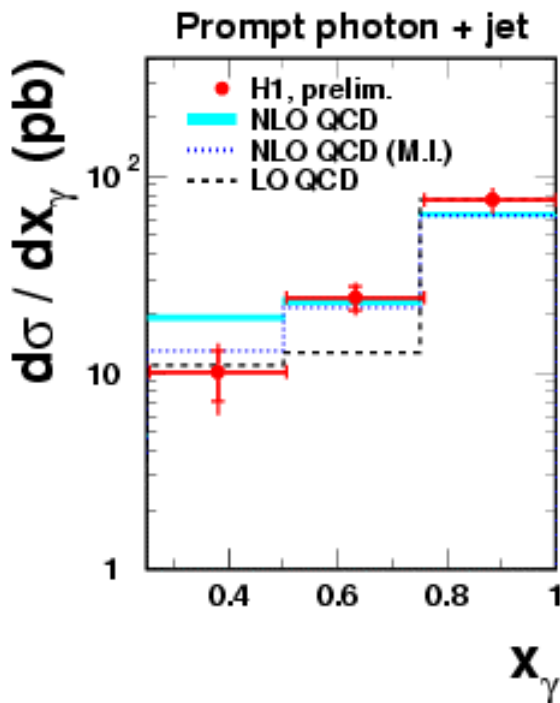


Data consistent within errors.

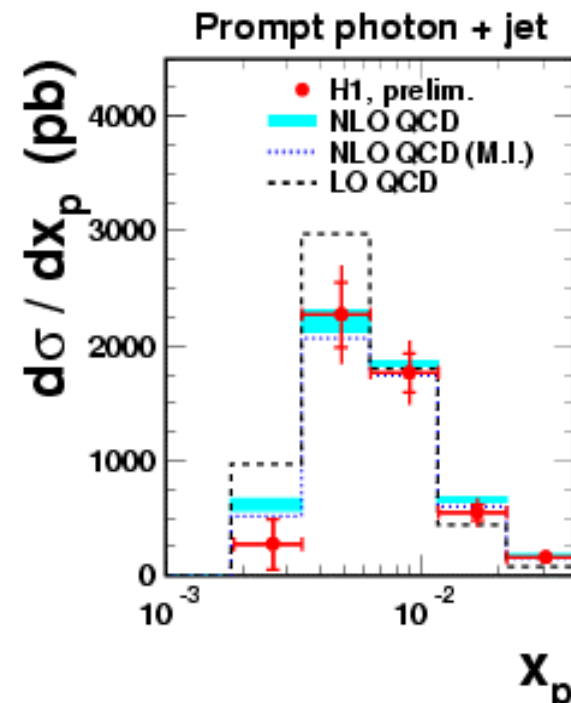
Photoproduction:

$(\gamma + \text{jet})$

σ vs. x_γ, x_p



$$x_\gamma = (E_T^{jet} e^{-\eta(jet)} + E_T^\gamma e^{-\eta(\gamma)}) / 2y E_e$$



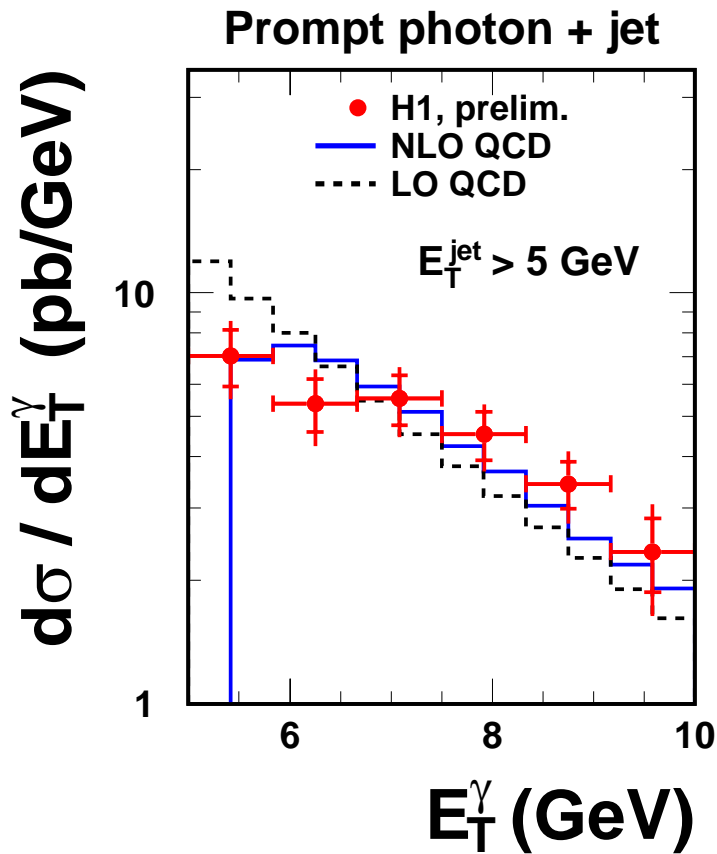
$$x_p = (E_T^{jet} e^{\eta(jet)} + E_T^\gamma e^{\eta(\gamma)}) / 2E_p$$

- Multiple interactions matter at $x_\gamma < 0.5$ (resolved γ region)
- NLO + MI describes the data

Photoproduction

$(\gamma + \text{jet})$

Avoid symmetric E_T cuts



Fontannaz *et al.:*

NLO infrared instabilities
with symmetric cuts *e.g.*

$$E_{T,\min}^{\text{jet}} = E_{T,\min}^\gamma = 5 \text{ GeV}$$

Unphysical drop in prediction
just above cut (similar to dijets)

γ signal extraction in ZEUS

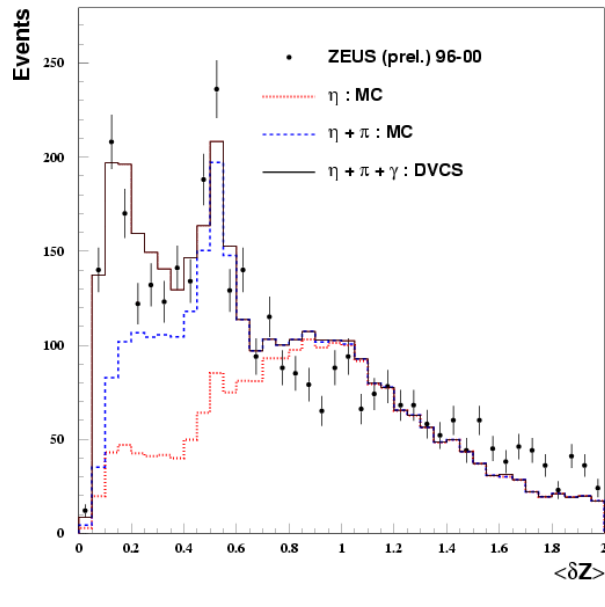
Shower shape variables for γ (from DVCS data), π^0, η (from MC)

Using 5 cm z-strips in Barrel e.m. calorimeter ($-0.7 < \eta < 0.9$)

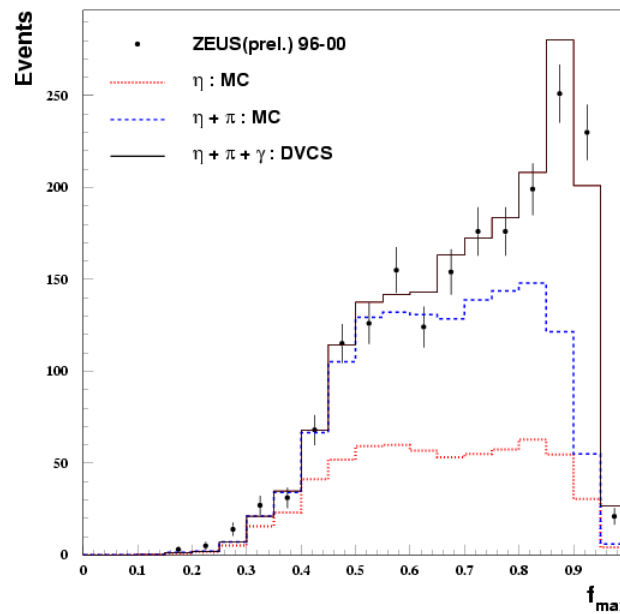
$$\delta Z = \sum_i E_i |Z_i - \langle Z \rangle| / \sum_i E_i$$

f_{max} = fraction of γ energy in highest cell

ZEUS



ZEUS



(use
 $\delta Z > 0.65$
only)

S/B~0.44

η fraction fixed from background at $\delta Z > 0.65$

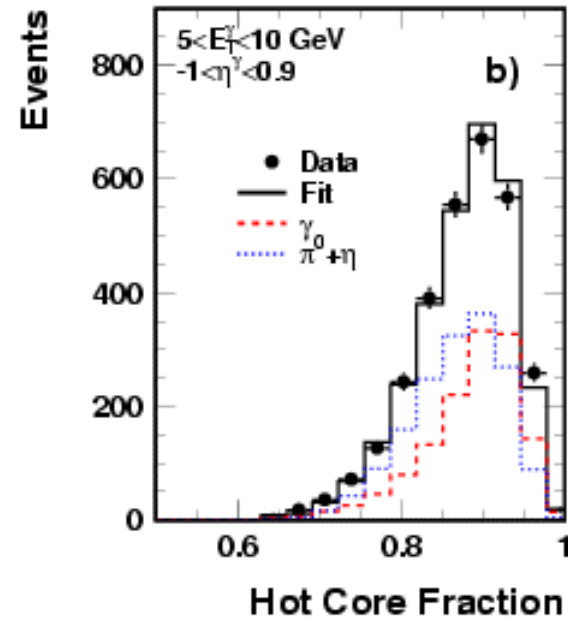
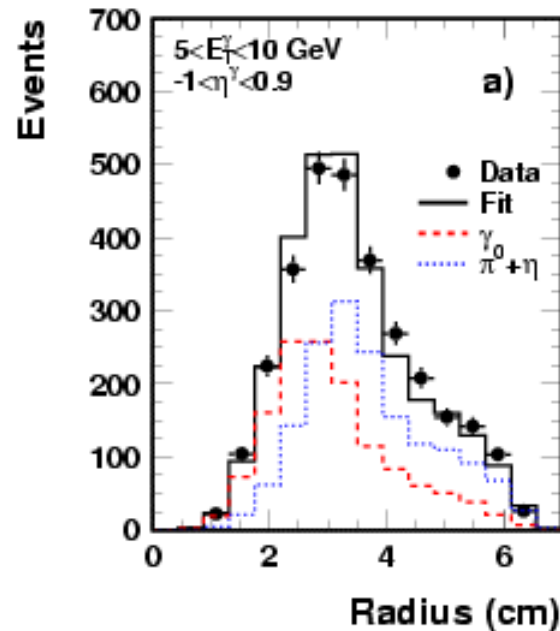
Background subtraction from f_{max} plot. Rather insensitive to errors in modelling showers (included in systematic errors)

γ signal extraction in H1

Use shower shape variables for γ , $(\pi^0 + \eta)$ (η fraction from MC)

$$Radius = \sum_{\text{cells}} w_i r_i / \sum_{\text{cells}} w_i$$

$$Hot \ core \ fraction = E_{\text{core}} / E_{\text{tot}}$$



Likelihood discriminator used in (E_T, η) bins to allow for energy dependence and varying calorimeter granularity.

- Shower shape variables well described.
- photoproduction S/B ~ 1